Supporting Information

for

Photocatalytic Substrate Oxidation Catalyzed by a Ruthenium(II) Complex with a Phenazine Moiety as the Active Site Using Dioxygen as a Terminal Oxidant

Tomoya Ishizuka,[†] Taichiro Nishi,[†] Nanase Namura,[†] Hiroaki Kotani,[†]

Yasuko Osakada,[§] Mamoru Fujitsuka,[§] Yoshihito Shiota,[‡] Kazunari

Yoshizawa,[‡, #] Takahiko Kojima[*, †]*

[†]Department of Chemistry, Graduate School of Pure and Applied Sciences, University of Tsukuba, 1-1-1 Tennoudai, Tsukuba, Ibaraki 305-8571, Japan

[§]SANKEN (The Institute of Scientific and Industrial Research), Osaka University, Ibaraki, Osaka 567-0047, Japan

[‡]Institute for Materials Chemistry and Engineering, Kyushu University, Moto-oka, Nishi-Ku, Fukuoka 819-0395, Japan

[#]Current Address: Fukui Institute for Fundamental Chemistry, Kyoto University, Sakyo-ku, Kyoto 606-8103, Japan

Experimental Section

General

Chemicals and solvents were used as received from commercial sources such as Tokyo Chemical Industry (TCI) Co., Wako Chemicals, Nacalai Tesque or Sigma-Aldrich Corp., unless otherwise mentioned. Complex **1**[1] and **1**'[2] was synthesized in accordance with the literature procedure.

NMR measurements were performed using a Bruker AVANCE-400 spectrometer. UV-vis absorption spectra were recorded using Shimadzu UV-3600 spectrophotometer. ESI-TOF-MS spectra were measured on a JEOL JMS-T100CS spectrometer. The photoirradiation of the sample was performed by using a Xe light source (300 W) of an ASAHI SPECTRA MAX-350 at room temperature.

Photocatalytic Substrate Oxidation

A substrate (100 mM) and a catalyst (0.2 mM) such as complex **1** were dissolved in D_2O (550 μL) and the solution was irradiated with a Xe lamp ($\lambda > 380$ nm) for 12 h under O_2 (0.1 MPa) or Ar. The reaction was monitored by ^1H NMR spectroscopy using DSS (= 2,2-dimethyl-2-silapentane-5-sulfonate sodium salt) as an internal standard to quantify the amount of product formed.

Iodometry

To a solution (2.0 mL) of NaI (1 M) in acetonitrile, a reaction solution (12.5 μL) was added, and the UV-vis spectrum was measured. The absorbance derived from I_3^- at 360 nm in the UV-vis spectrum was used to calculate the amount of H_2O_2. In the calculation, the absorbance was corrected by subtraction of the absorbance of the sample at 360 nm prepared by addition of the solution before photo-irradiation as the background.

Quantification of H_2O_2 by TiTPyP

At first, TiTPyP (1.70 mg, 1.25 μmol) was dissolved in HCl aq (0.05 M, 25 mL) to obtain a TiTPyP solution. A standard solution of H_2O_2 (0.10 M) was also prepared by diluting 30% v/v H_2O_2 aq (5.5 mL) to 500 mL with de-ionized water. To a sample solution (0.2 mL) in water, were added 5.0 M $HClO_4$ aq (0.2 mL) and the TiTPyP solution (0.2 mL). The mixed solution was then allowed to stand for 5 min at room temperature. The solution was further diluted to 2.0 mL with de-ionized water and the absorbance at 432 nm was measured. A blank solution was also prepared in a similar manner, using distilled water instead of the sample solution. The difference of the absorbance at 432 nm between the sample and blank solutions was used to determine the H_2O_2 concentration.

Determination of Quantum Yields.

To an aqueous solution (2 mL) of **1**-H^+, whose pH was adjusted to be 1.3 by addition of TfOH, BnOH (50 mM) was added and the atmosphere was replaced with Ar

by its bubbling through the solution for 10 min. The solution was photo-irradiated with a Xe lamp, equipped with a band-path filter (λ_{center} = 380 nm), and the conversion from **1**-H^+ to **2**-H^+ was monitored by UV-Vis spectroscopy. Based on the absorbance change at 375 nm, the concentration of **2**-H^+ ([**2**-H^+]) at a moment was estimated and [**2**-H^+] was plotted against the irradiation time to determine the initial reaction rate of the formation of **2**-H^+ (Figure S13). Using the light intensity of the Xe lamp at 380 nm, preliminarily determined by the actinometer method,[3] the quantum yield (Φ) for formation of **2**-H^+ was determined based on the following equation.

$$\Phi = \Delta n / I \qquad \text{(S1)}$$

Δn: production rate of **2**-H^+ (mol s^{-1}). I: intensity of incident light (einstein s^{-1}).

Determination of the Association Constants between 1-H^+ and BnOH.

A solution of **1**-H^+ (50 μM) in D_2O, whose pD was adjusted by addition of TfOH to be 1.3, was titrated with BnOH at 298 K, and the solution was monitored by ^{1}H NMR spectroscopy. The chemical shift change was analyzed by the following equation.[4]

$$\Delta\delta_{obs} = [(1 + K_{11}[H]_0 + K_{11}[G]_0) - \{(1 + K_{11}[H]_0 + K_{11}[G]_0)^2 - 4K_{11}^2[G]_0[H]_0\}^{1/2}] \times \Delta\delta_{11}/(2K_{11}[H]_0) \qquad \text{(S2)}$$

$\Delta\delta_{obs}$: chemical shift of the observed signal, K_{11}: association constant between **1**-H^+ and BnOH, $[H]_0$: concentration of **1**-H^+, $[G]_0$: concentration of BnOH, $\Delta\delta_{11}$: chemical shift for the 1:1 adduct.

X-ray Diffraction Analysis.

A single crystal of [**1**-H^+]·$(OTf)_3$ suitable for X-ray crystallography was obtained by recrystallization form an aqueous solution of **1**-H^+, whose pH was controlled by addition of TfOH. The crystal was mounted using a mounting loop. All diffraction data were collected on a Bruker APEXII diffractometer at 120 K with a graphite-monochromated Mo Kα radiation source (λ = 0.71073 Å) by the ω scan. The structure was solved by a direct method (SIR-97)[5] and expanded with a differential Fourier technique. All non-hydrogen atoms were refined anisotropically and the refinement was carried out with full-matrix least-squares on F. All calculations were performed using the Yadokari-XG crystallographic software package.[6] Crystallographic data for [**1**-H^+]·$(OTf)_3$ are summarized in Table S3.

DFT Calculations.

Density functional theory (DFT) and time-dependent density functional theory (TD-DFT)[7] calculations were performed by using the Gaussian 16 program packeages.[8] The method of choice is the B3LYP-D3 level of theory[9-11] combined with the SDD basis set[12] for the Ru atom and the D95** basis set[13] for the other atoms. Solvent effects of water

(dielectric constant = 78.36) were considered by using the polarizable continuum model (PCM)[14] in the DFT calculations. First, we optimized the complex of BnOH and **1**-H^+ (Table S4). After that, we performed TD-DFT calculations using the optimized structure. To analyze the electronic distribution of the excited states, the electron density difference maps were visualized by using the GaussSum 3.0 program.[15]

Reference and Notes

1. Li, J.; Wei, Y.; Chen, X.-Y.; Zhu, Z.-L.; Gao, Y. *Inorg. Chem. Commun.* **2017**, *86*, 10.
2. Müller, C.; Friedländer, I.; Bagemihl, B.; Rau, S.; Dietzek-Ivanšić, B. *Phys. Chem. Chem. Phys.*, **2021**, *23*, 27397.
3. Lee, J.; Selinger, H.-H. *J. Chem. Phys.* **1964**, *40*, 519.
4. Kano, K.; Kitae, T.; Shimofuri, Y.; Tanaka, N.; Mineta, Y. *Chem.–Eur. J.* **2000**, *6*, 2705-2713.
5. Sheldrick, G. M. *SIR97 and SHELX97, Programs for Crystal Structure Refinement*, University of Göttingen, Göttingen (Germany), 1997.
6. Kabuto, C.; Akine, S.; Nemoto, T.; Kwon. E. Release of Software (Yadokari-XG 2009) for Crystal Structure Analyses. *J. Cryst. Soc. Jpn.* **2009**, *51*, 218-224.
7. Casida, M. E.; C. Jamorski, C.; Casida, K. C.; Salahub, D. R. *J. Chem. Phys.* **1998**, *108*, 4439-4449.
8. Gaussian 16, Revision C.01, Frisch, M. J.; Trucks, G. W.; Schlegel, H. B.; Scuseria, G. E.; Robb, M. A.; Cheeseman, J. R.; Scalmani, G.; Barone, V.; Petersson, G. A.; Nakatsuji, H.; Li, X.; Caricato, M.; Marenich, A. V.; Bloino, J.; Janesko, B. G.; Gomperts, R.; Mennucci, B.; Hratchian, H. P.; Ortiz, J. V.; Izmaylov, A. F.; Sonnenberg, J. L.; Williams-Young, D.; Ding, F.; Lipparini, F.; Egidi, F.; Goings, J.; Peng, B.; Petrone, A.; Henderson, T.; Ranasinghe, D.; Zakrzewski, V. G.; Gao, J.; Rega, N.; Zheng, G.; Liang, W.; Hada, M.; Ehara, M.; Toyota, K.; Fukuda, R.; Hasegawa, J.; Ishida, M.; Nakajima, T.; Honda, Y.; Kitao, O.; Nakai, H.; Vreven, T.; Throssell, K.; Montgomery, J. A., Jr.; Peralta, J. E.; Ogliaro, F.; Bearpark, M. J.; Heyd, J. J.; Brothers, E. N.; Kudin, K. N.; Staroverov, V. N.; Keith, T. A.; Kobayashi, R.; Normand, J.; Raghavachari, K.; Rendell, A. P.; Burant, J. C.; Iyengar, S. S.; Tomasi, J.; Cossi, M.; Millam, J. M.; Klene, M.; Adamo, C.; Cammi, R.; Ochterski, J. W.; Martin, R. L.; Morokuma, K.; Farkas, O.; Foresman, J. B.; Fox, D. J. Gaussian, Inc., Wallingford CT, 2016.
9. Becke, A. D. *Phys. Rev. A* **1988**, *38*, 3098 -3100.
10. Lee, C.; Yang, W.; Parr, R. G. *Phys. Rev. B: Condens. Matter Mater. Phys.* **1988**, *37*, 785-789.
11. S. Grimme, S.; Antony, J.; Ehrlich, S.; Krieg, H. *J. Chem. Phys.* **2010**, *132*, 154104.
12. Andrae, D.; Häußermann, U.; Dolg, M.; Stoll, H.; Preuß, H. *Theor. Chem. Acc.* **1990**, *77*, 123-141.

13. Dunning T. H.; Hay, P. J. *Modern Theoretical Chemistry*, Schaefer, H. F. III Plenum, New York, 1976, vol. 3, 1–27.
14. J. Tomasi, J.; Mennucci, B.; Cammi, R. *Chem. Rev.* **2005**, *105*, 2999-3094.
15. O'Boyle, N. M.; Tenderholt, A. L.; Langner, K. M. *J. Comput. Chem.* **2008**, *29*, 839-845.

Scheme S1. A proposed reaction mechanism of BnOH oxidation by $^1O_2$ formed through energy transfer

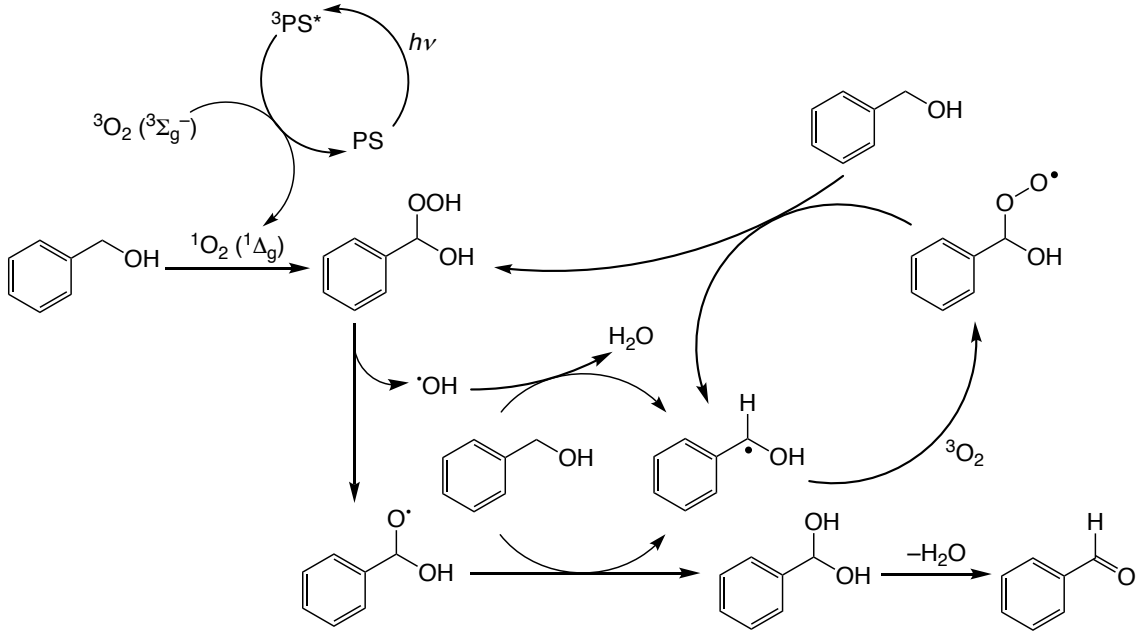

Scheme S2. A proposed reaction mechanism for cBuOH oxidation by $^1O_2$ formed through the photosensitization

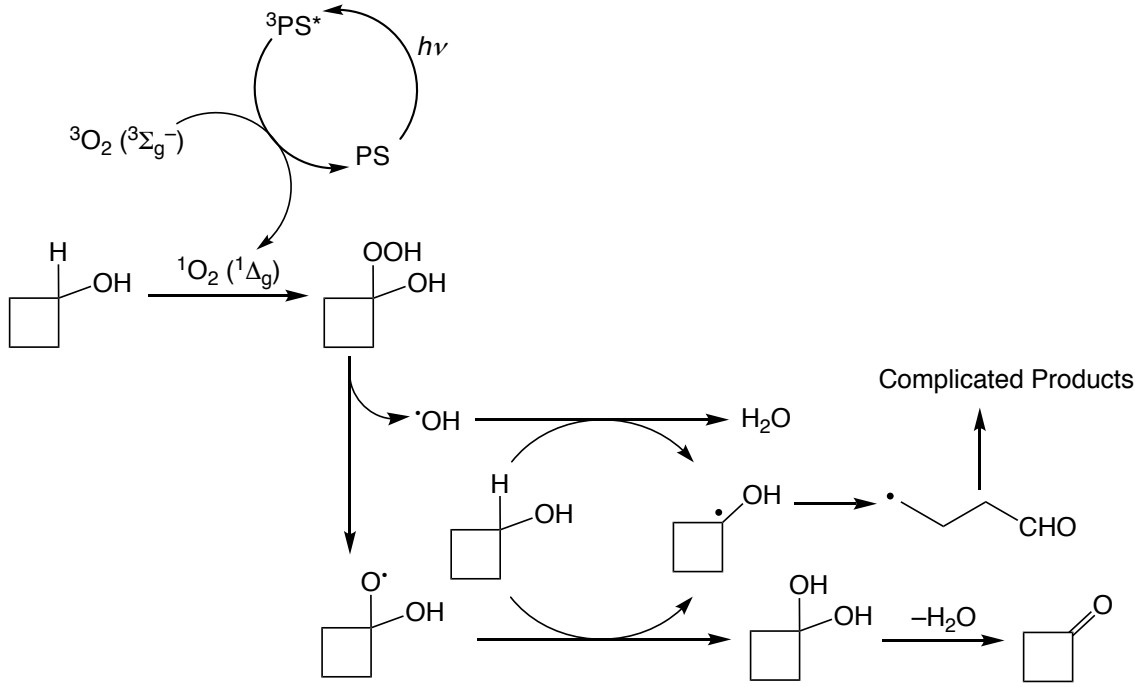

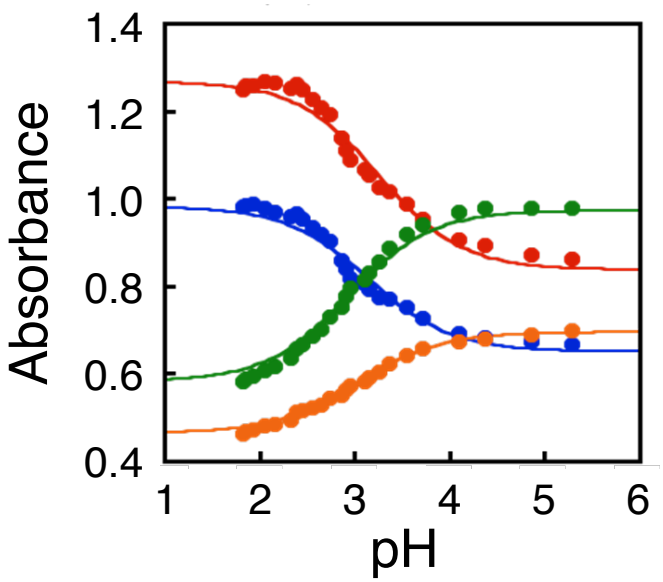

Figure S1. pH-dependent absorbance changes of **1** at 356 nm (blue-filled circles), 375 nm (red-filled circles), 384 nm (green-filled circles), and 393 nm (orange-filled circles). The fitting curves are provided based on eqn S3 shown below.

$$A = A_0 - (A_1 - A_0)/(K_a \times 10^{-pH} + 1) \quad \text{(S3)}$$

A_0: absorbance of the protonated species (**1**-H^+) at a wavelength. A_1: absorbance of the non-protonated species (**1**) at the wavelength. K_a: acid dissociation constant.

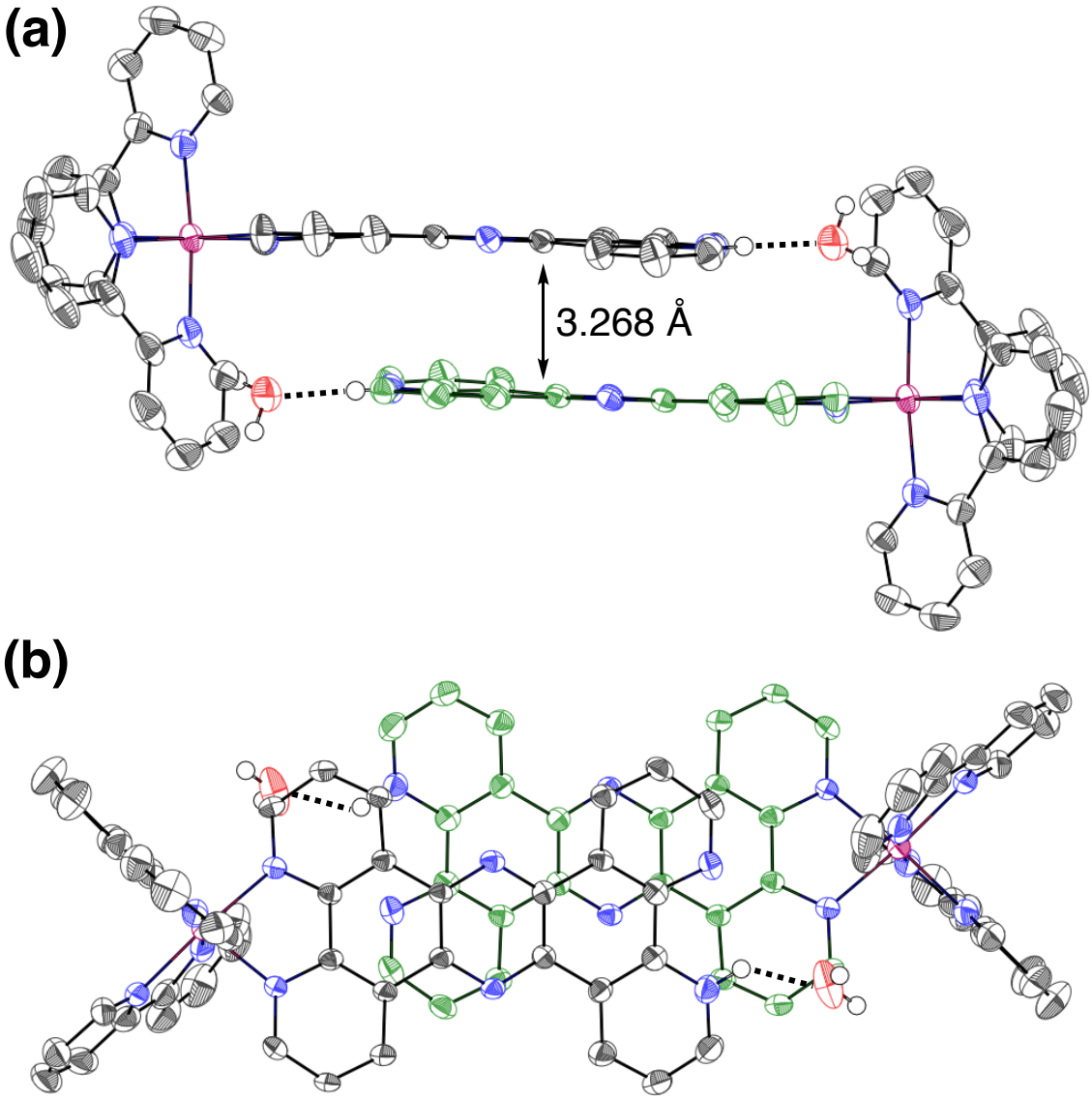

Figure S2. ORTEP drawings for the π-stacked dimer of **1**-H^+ in the crystal: (a) A side view, (b) a top view. Carbon atoms of the tpphz ligand in the second layer are colored in green for clarity.

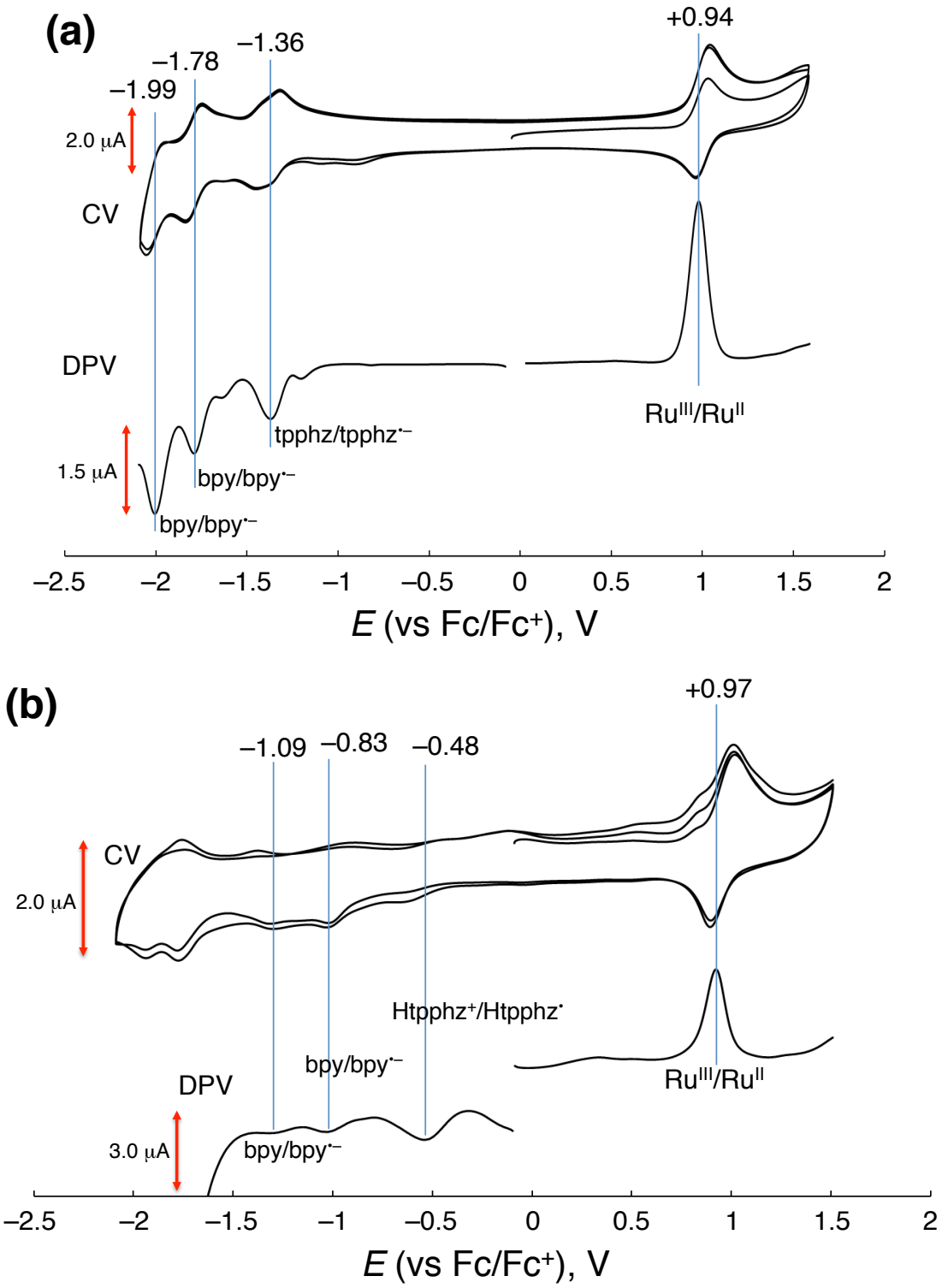

Figure S3. Cyclic and differential-pulse voltammograms (CV and DPV) of **1** (a) and **1**-H^+ (b) in CH_3CN, containing $TBAPF_6$ (0.1 M) as an electrolyte, at room temperature. For the protonation of **1**, TfOH (0.5 mM) was added in (b). WE: glassy carbon disk, CE: Pt wire, RE: $Ag/AgNO_3$.

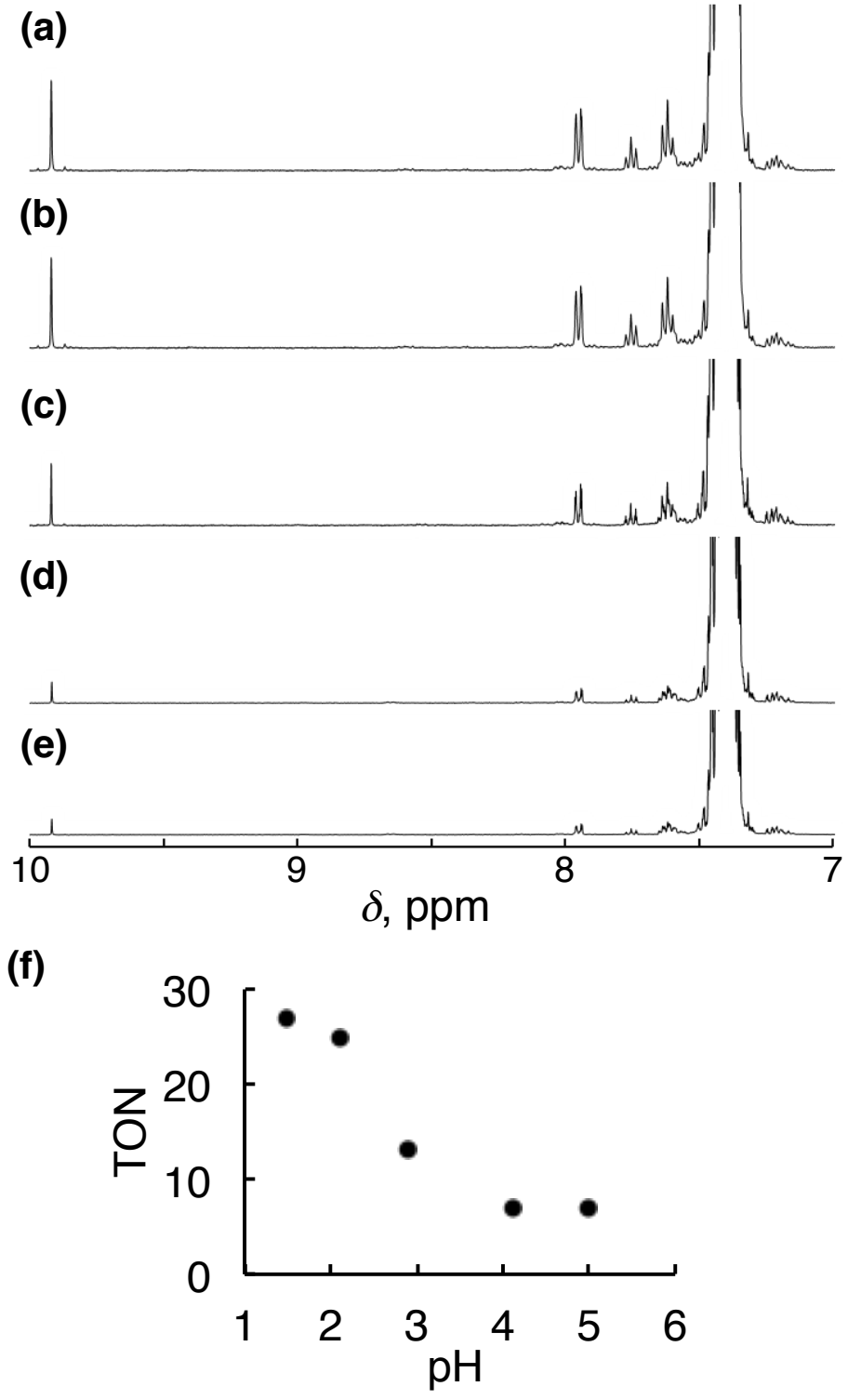

Figure S4. ^{1}H NMR spectra of the reaction mixture for the BnOH (100 mM) oxidation by **1** (0.1 mM) in B.-R.-buffered D_2O, whose pD was adjusted to be 1.5 (a), 2.0 (b), 3.0 (c), 4.0 (d) and 5.0 (e), under O_2 (1 atm) after white-light irradiation for 10 h. (f) A plot of the TONs for the PhCHO formation, obtained from (a) – (e), against the solution pD.

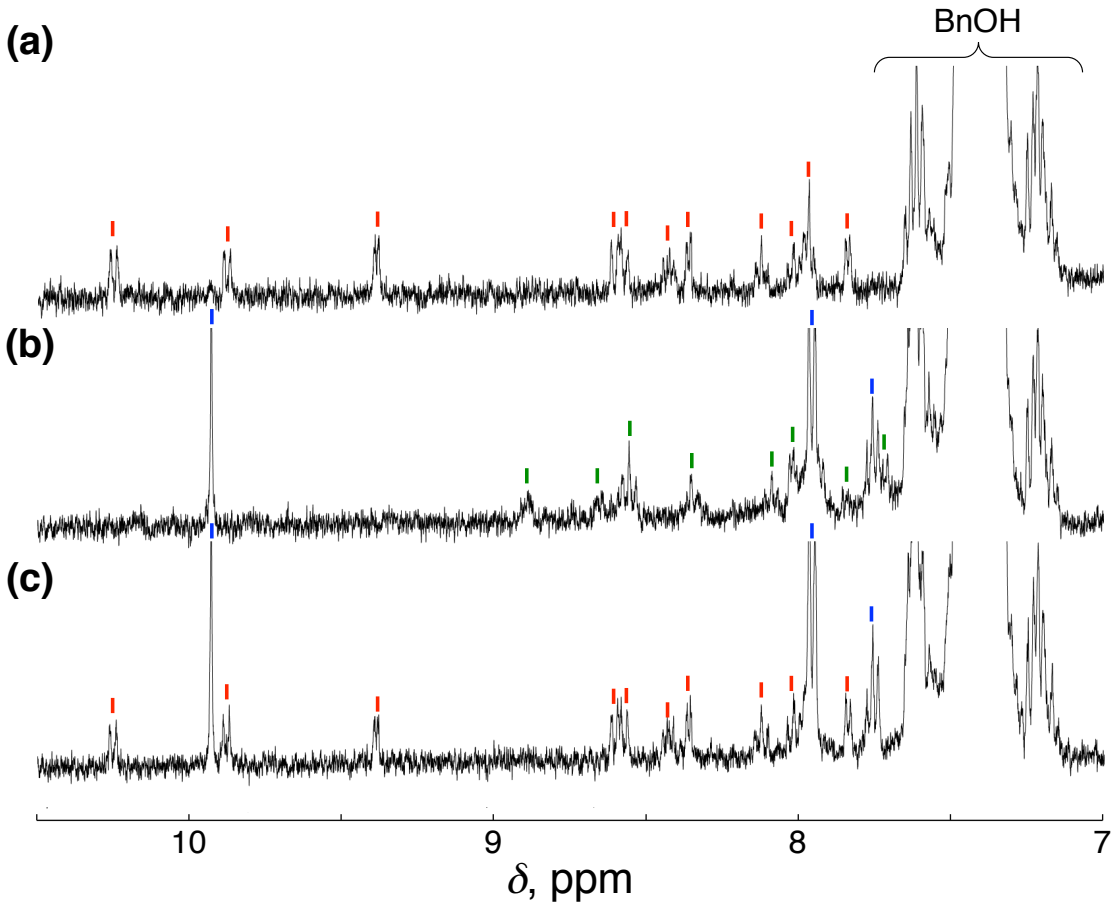

Figure S5. (a) ^{1}H NMR spectrum of **1**-H^{+} (100 μM) in D_2O, whose pH was adjusted to be 1.3 by addition of TfOH, containing BnOH (50 mM) under Ar. (b) ^{1}H NMR spectrum after photoirradiation ($\lambda > 380$ nm) for 1 h to a solution of (a) to afford **2**-H^{+} and PhCHO as photo-products. (c) ^{1}H NMR spectrum after addition of O_2 (200 μL) to the headspace of the solution of (a) to revert **2**-H^{+} to **1**-H^{+}. The ^{1}H NMR signals of **1**-H^{+}, **2**-H^{+} and PhCHO are indicated by red, green and blue sticks, respectively.

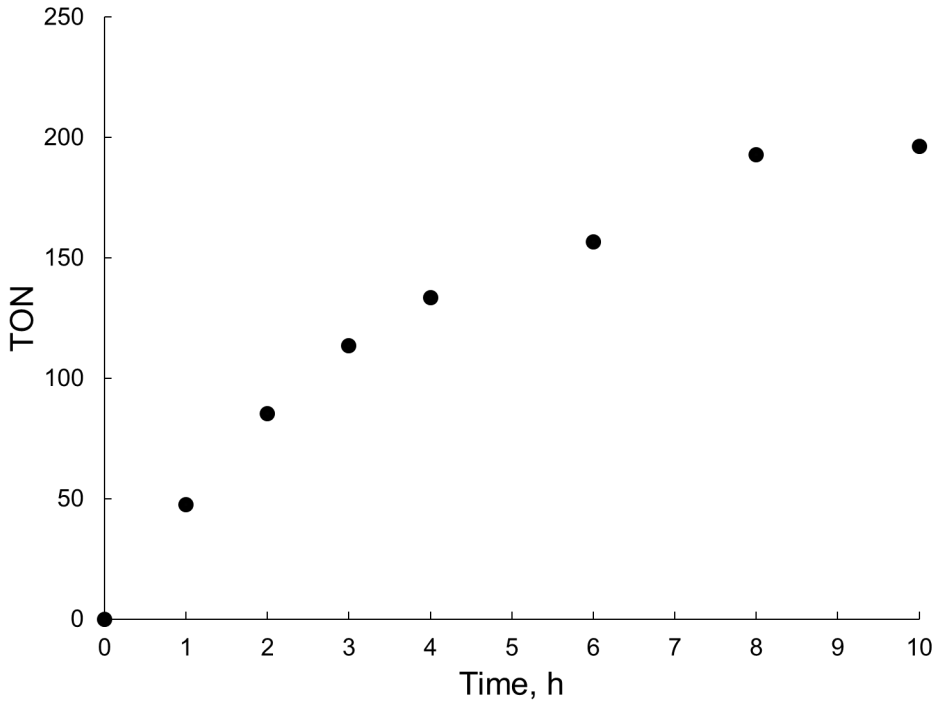

Figure S6. Time course of TON of the PhCHO production in the photocatalytic BnOH oxidation by **1**-H^+. TON = [PhCHO]/[**1**-H^+]$_0$. Solvent: B.-R.-buffered D_2O (pD = 1.5). Light source: Xe lamp ($\lambda > 380$ nm). Atmosphere: O_2 (1 atm). T = room temperature. [**1**-H^+]$_0$ = 10 μM.

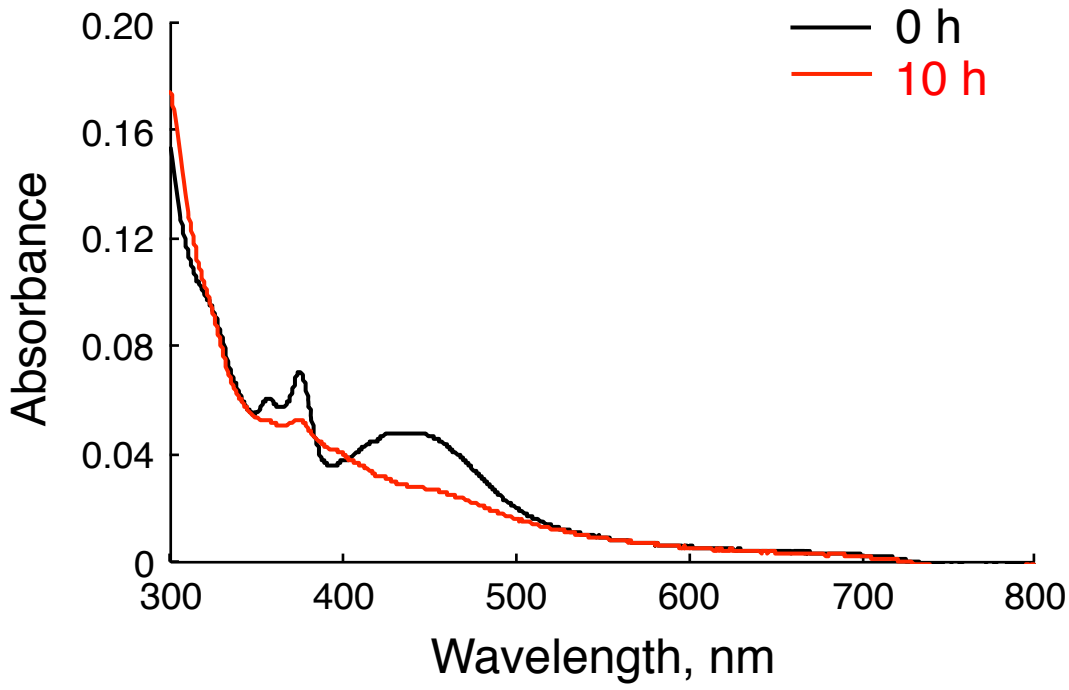

Figure S7. UV-Vis spectra of **1**-H^+ (50 μM) in B.-R.-buffered D_2O (pD = 1.5) before (black) and after (red) photocatalytic oxidation of BnOH (100 mM) for 10 h under white-light irradiation ($\lambda > 380$ nm) and O_2 atmosphere (0.1 MPa).

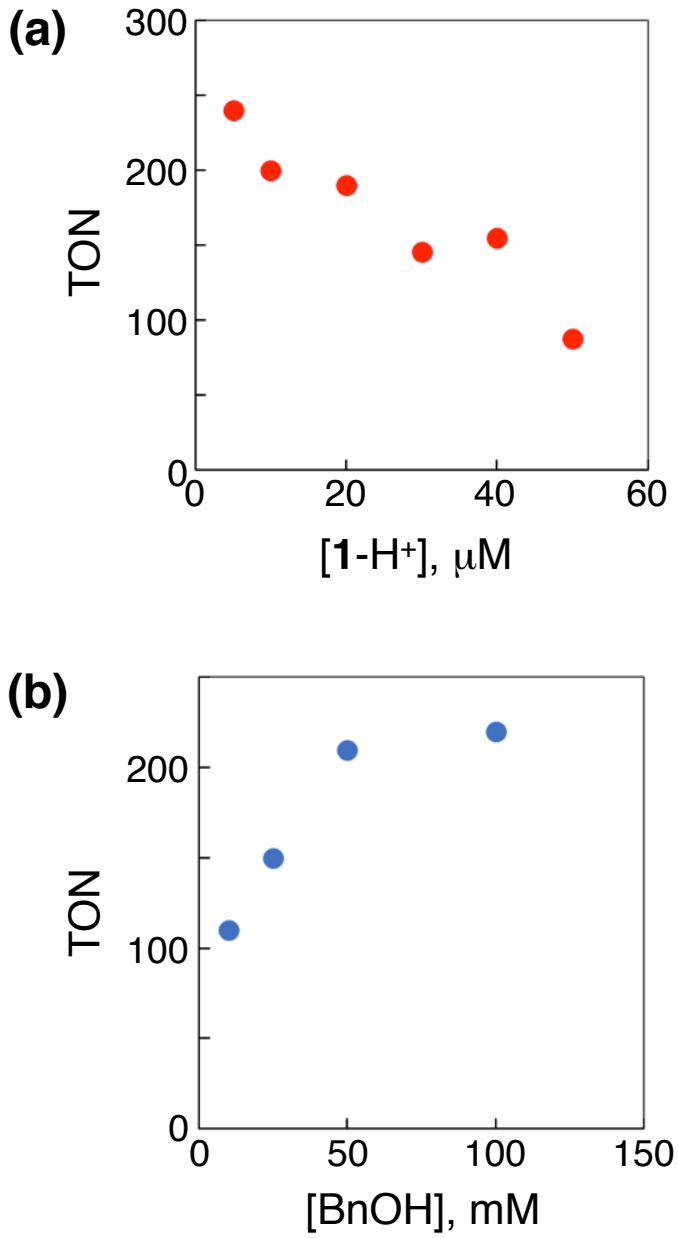

Figure S8. Dependence of TONs for the photocatalytic PhCHO formation by **1**-H^+ on the concentration of **1**-H^+ (a) and on that of BnOH (b). TON = [PhCHO]/ [**1**-H^+]$_0$. Solvent: B.-R.-buffered D_2O (pD = 1.5). Reaction time: 10 h. Light source: Xe lamp ($\lambda > 380$ nm). Atmosphere: O_2 (1 atm). T = room temperature. [BnOH] = 100 mM for (a) and [**1**-H^+] = 10 μM for (b), respectively.

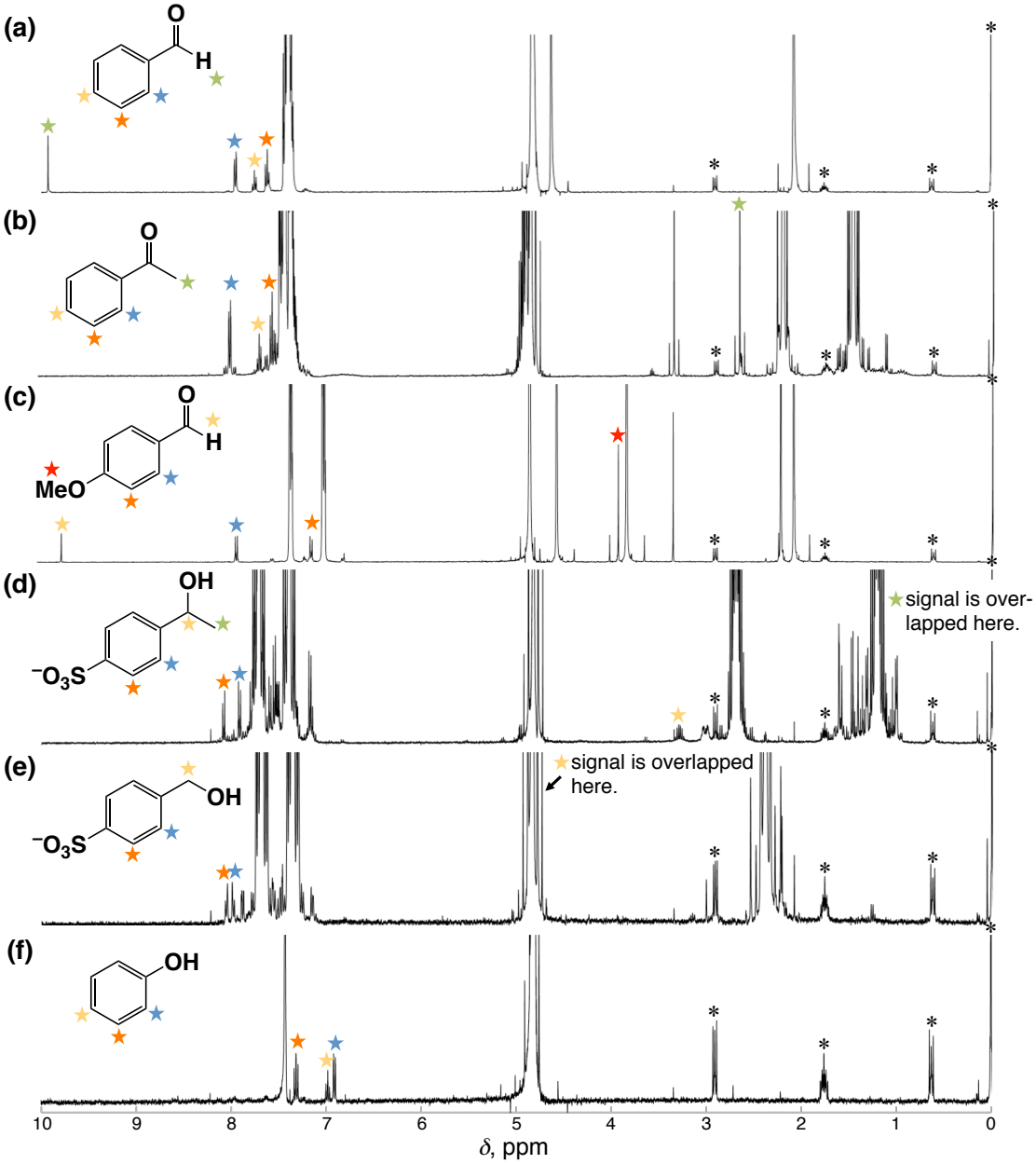

Figure S9. ^{1}H NMR spectra of the reaction mixtures after the photocatalytic oxidation of various substrates (50 mM) by **1**-H^{+} in B.-R.-buffered D_2O (pD = 1.5) at room temperature. Reaction time: 10 h. Substrates: BnOH (a), 1-phenyl-ethanol (b), 4-methoxy-benzyl alcohol (c), sodium *p*-ethylbenzene-sulfonate (d), sodium *p*-toluene-sulfonate (e), and benzene (f). Light source: Xe lamp ($\lambda > 380$ nm) for (a)–(c), or an LED lamp ($\lambda_{center} = 365$ nm) for (d)–(f). Asterisks (*) denote signals derived from DSS.

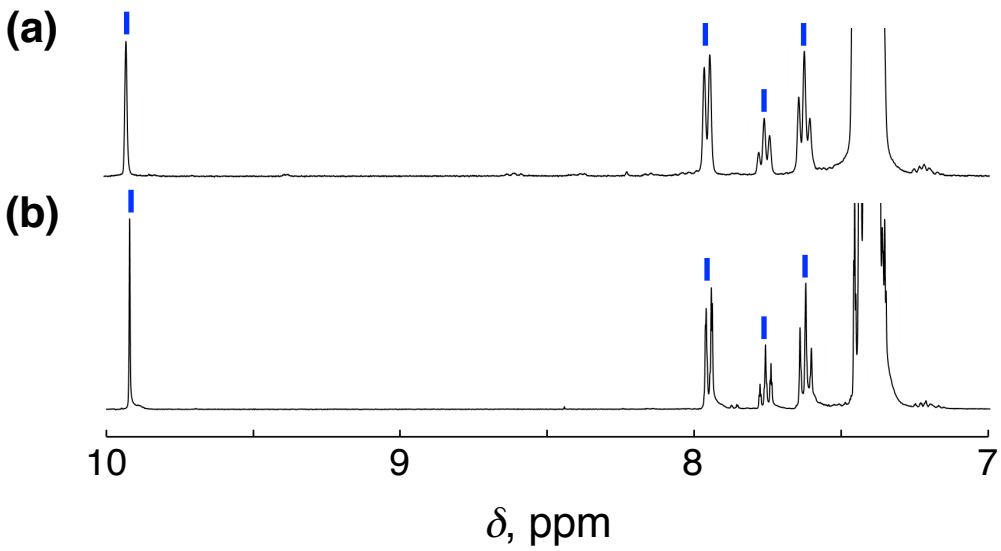

Figure S10. ^{1}H NMR spectra of reaction solutions for the photocatalytic BnOH oxidation by **1**-H^{+} under photo-irradiation (Xe lamp; $\lambda > 380$ nm) and O_2 (1 atm) in the absence (a) and presence (b) of NaN_3 (200 mM) as a singlet-oxygen scavenger. Reaction conditions: [**1**-H^{+}] = 0.1 mM, [BnOH] = 100 mM, T = room temperature. Solvent: B.-R.-buffered D_2O (pD = 1.5). Reaction time: 12 h. The ^{1}H NMR signals of PhCHO are indicated by blue sticks. The calculated TONs are 32 for (a) and 49 for (b), respectively.

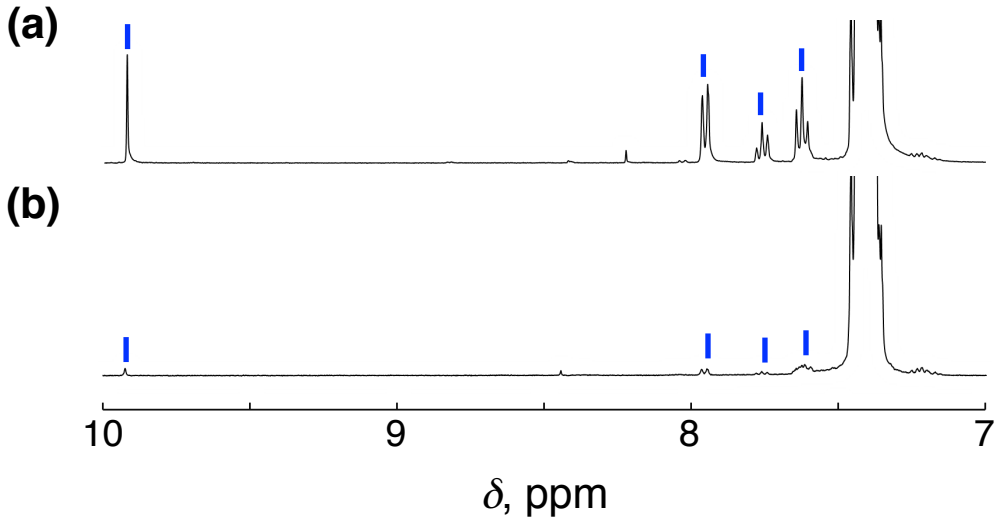

Figure S11. ^{1}H NMR spectra of reaction solutions for the photocatalytic BnOH oxidation by $[Ru(bpy)_3]Cl_2$ under photo-irradiation (Xe lamp; $\lambda > 380$ nm) and O_2 (1 atm) in the absence (a) and presence (b) of NaN_3 (200 mM) as a singlet-oxygen scavenger. Reaction conditions: $[[Ru(bpy)_3]^{2+}] = 0.1$ mM, [BnOH] = 100 mM, T = room temperature. Solvent: B.-R.-buffered D_2O (pD = 1.5). Reaction time: 12 h. The ^{1}H NMR signals of PhCHO are indicated by blue sticks. The calculated TONs are 33 for (a) and 2 for (b), respectively.

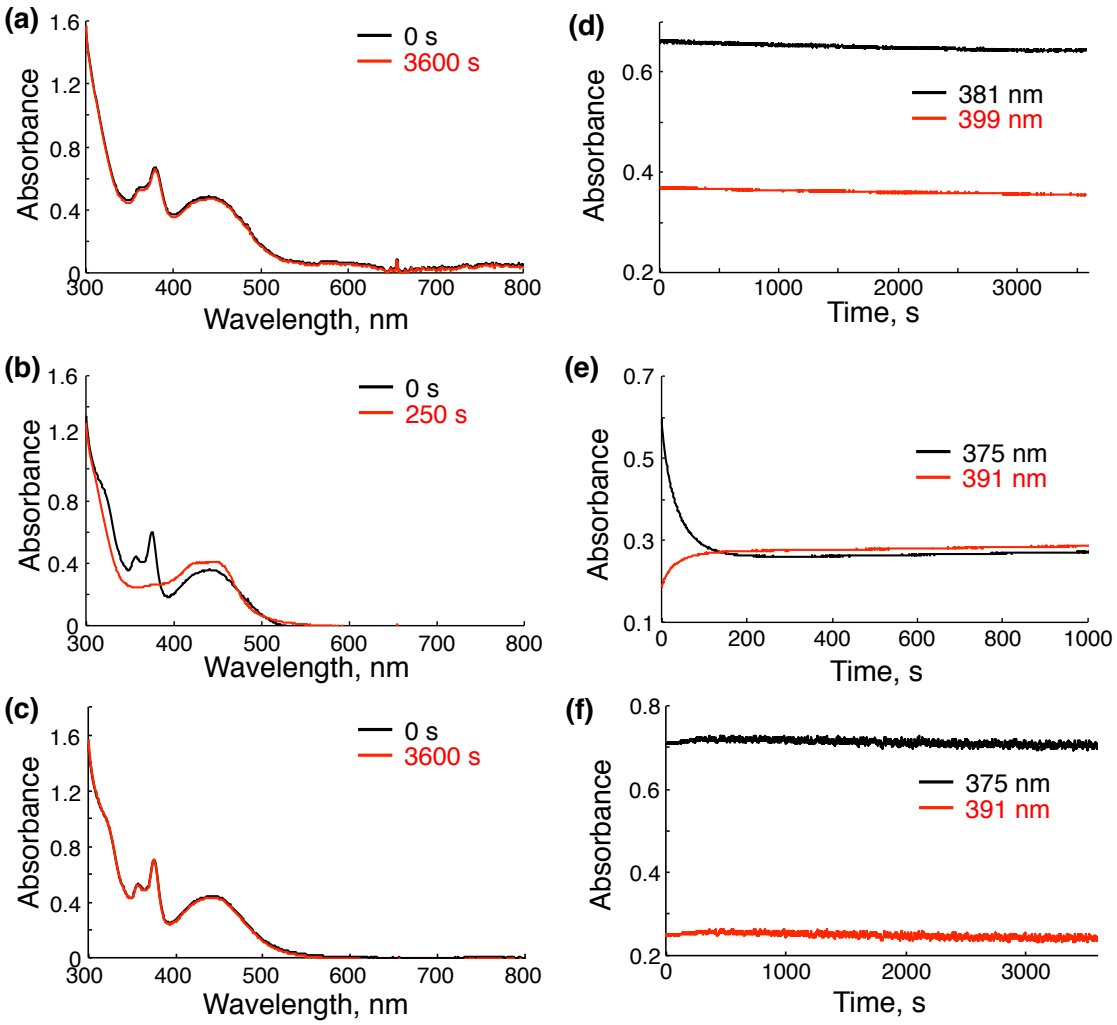

Figure S12. UV-Vis spectral changes (a, b, c) upon photoirradiation to an aqueous solution of **1** (25 μM) and BnOH (50 mM) at 297 K under Ar (1 atm) and the plots of the absorbance changes at specific wavelengths against the irradiation time (d, e, f). In the case of b, c, e, and f, the aqueous solutions contained TfOH (50 mM) and thus the pH of the solutions was 1.3. On the other hand, the solution used for a and d did not contain any acids and its pH was 7.0. Light source: Xe lamp. Irradiation wavelength, $\lambda > 380$ nm (a, b, d and e), and $\lambda = 440$ nm (c and f) using a band-path filter.

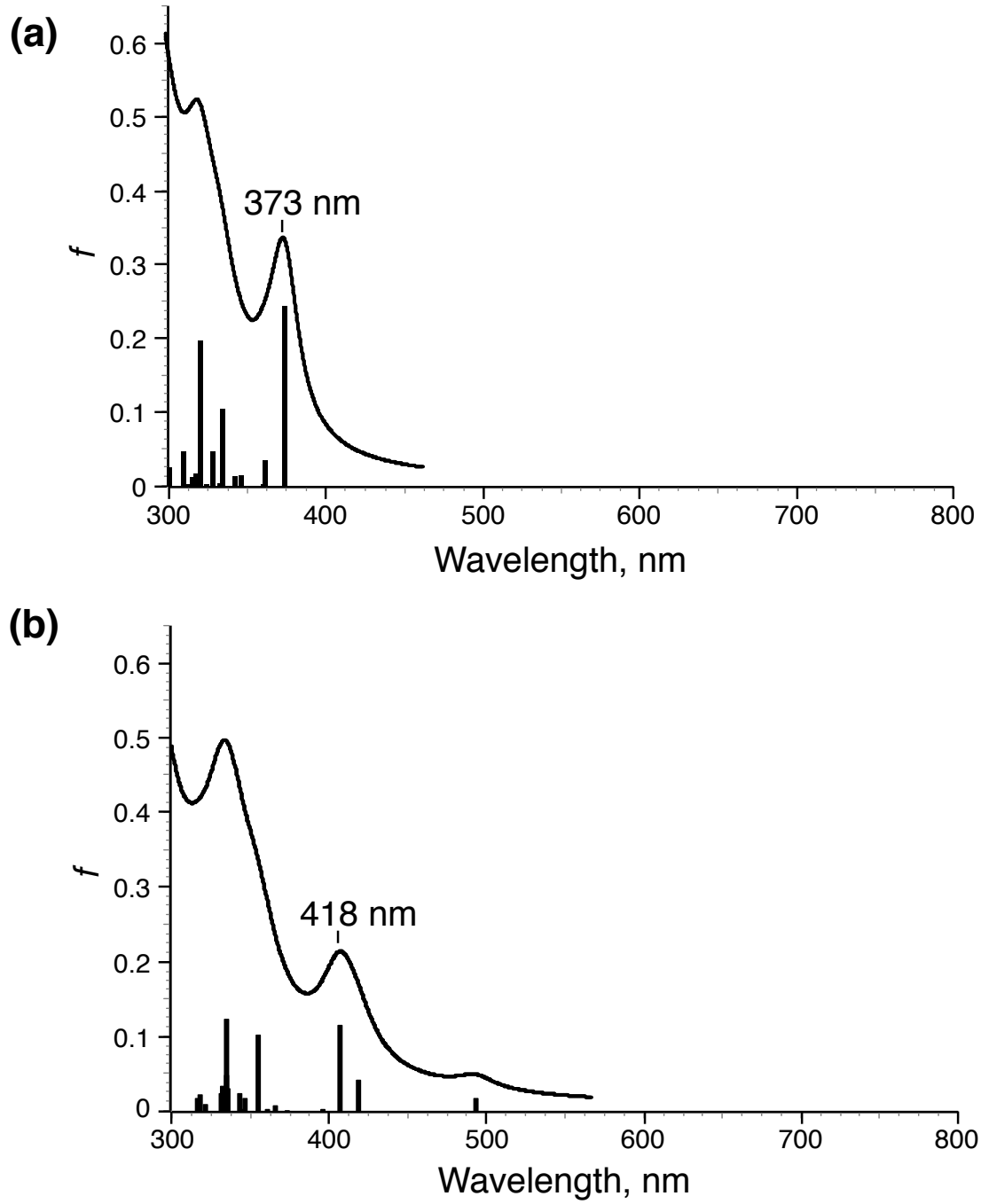

Figure S13. Simulated UV-Vis spectra of **1**-H^+ (a) and **2**-H^+ (b) based on the TD-DFT calculations.

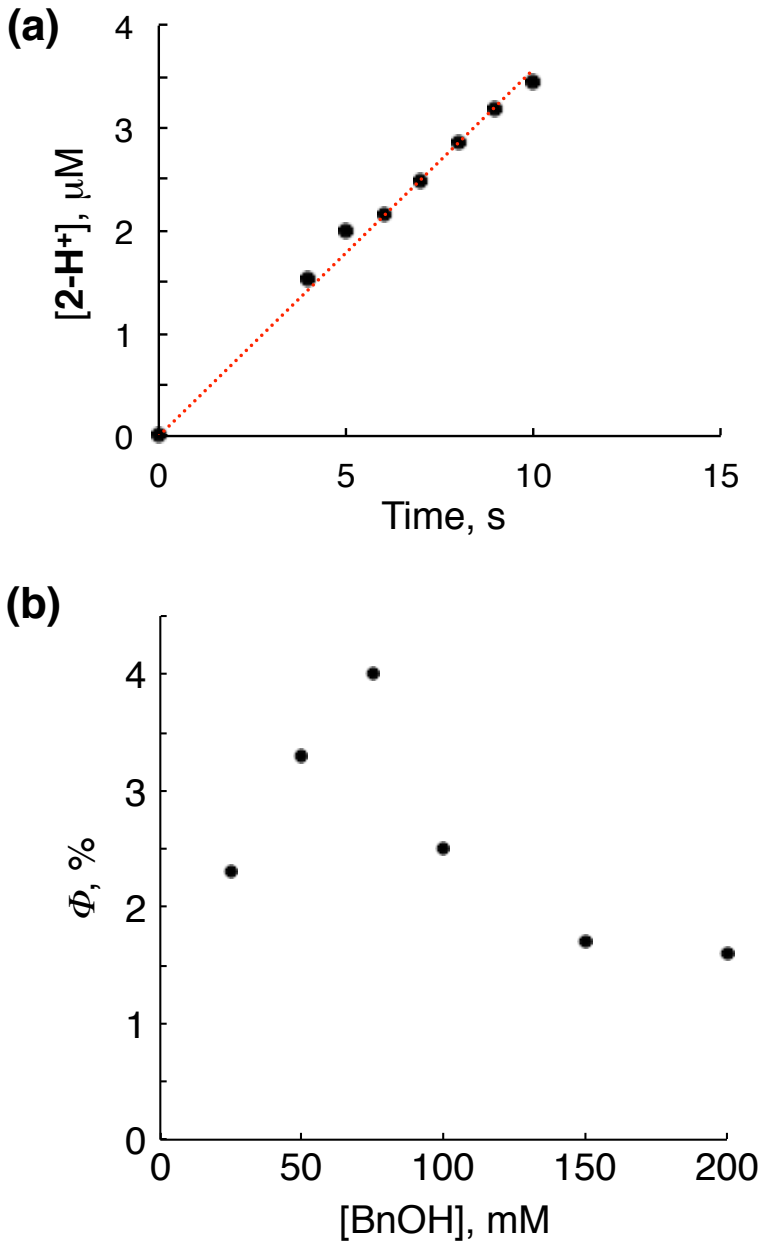

Figure S14. Time course for the formation of **2**-H^+ from **1**-H^+ in H_2O at pH = 1.3, adjusted by addition of TfOH, in the presence of BnOH (50 mM), with light irradiation at 380 nm under Ar. The concentration of **2**-H^+ was determined based on the absorbance at 375 nm and the absorption coefficients of **1**-H^+ and **2**-H^+ at the wavelength. From the slope of the plot, the initial rate for the formation of **2**-H^+ was determined to be 0.35 μM s^{-1}. (b) Dependence of the quantum yields, Φ, of photochemical formation of **2**-H^+ on the concentration of BnOH under the conditions described in (a).

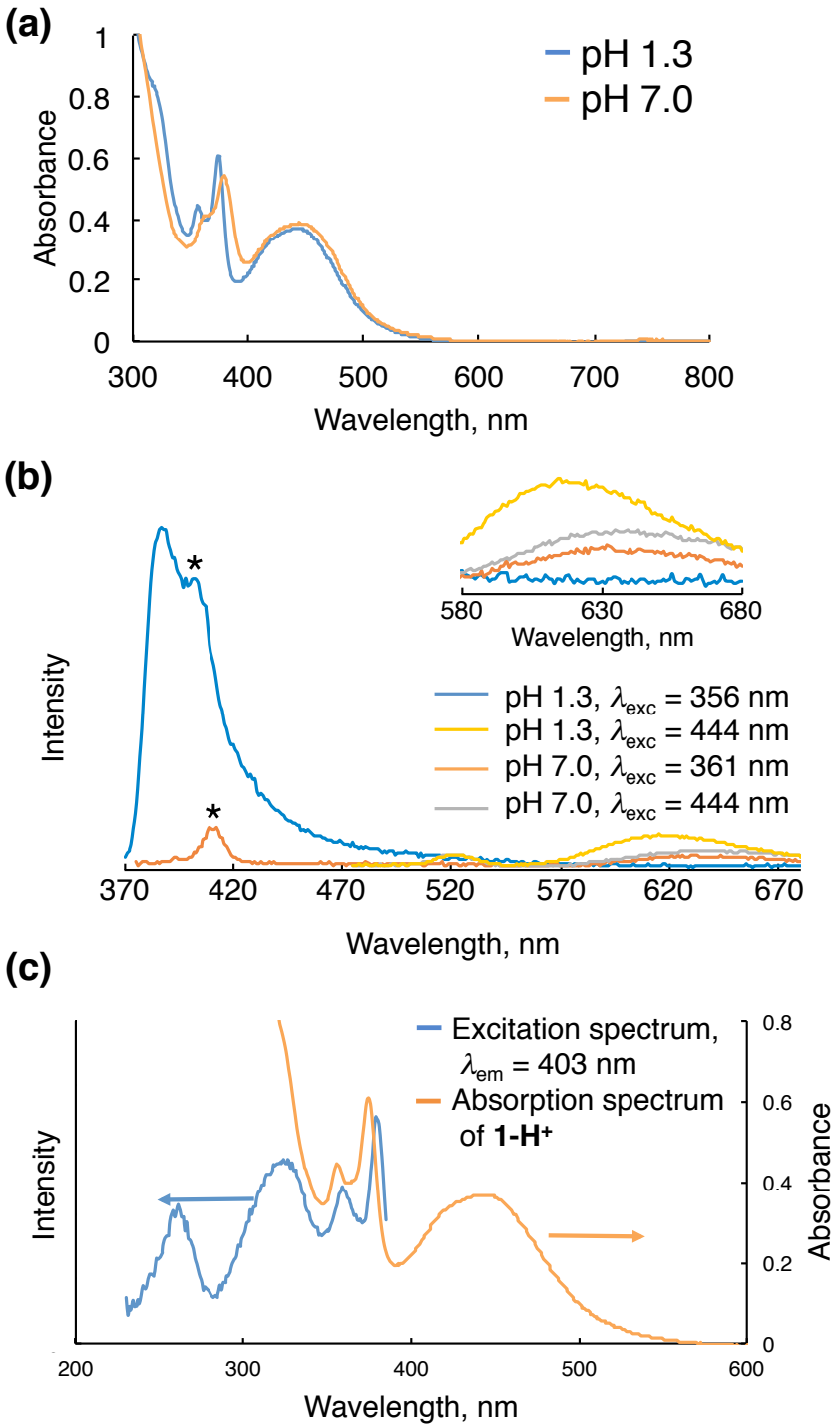

Figure S15. (a) UV-Vis spectra of **1** in H_2O at pH = 7.0 (orange) and **1**-H^+ in H_2O at pH = 1.3, adjusted by addition of TfOH (blue). (b) Emission spectra of **1** in H_2O at pH = 7.0 with excitation wavelength at 361 (orange) and 444 nm (gray) and **1**-H^+ in H_2O at pH = 1.3 with excitation wavelength at 356 nm (blue) and 444 nm (yellow). (c) An excitation spectrum of **1**-H^+ in H_2O at pH = 1.3 monitoring at 403 nm (blue) and an absorption spectrum of **1**-H^+ in H_2O at pH = 1.3 (orange). *: Raman scattering of the incident light.

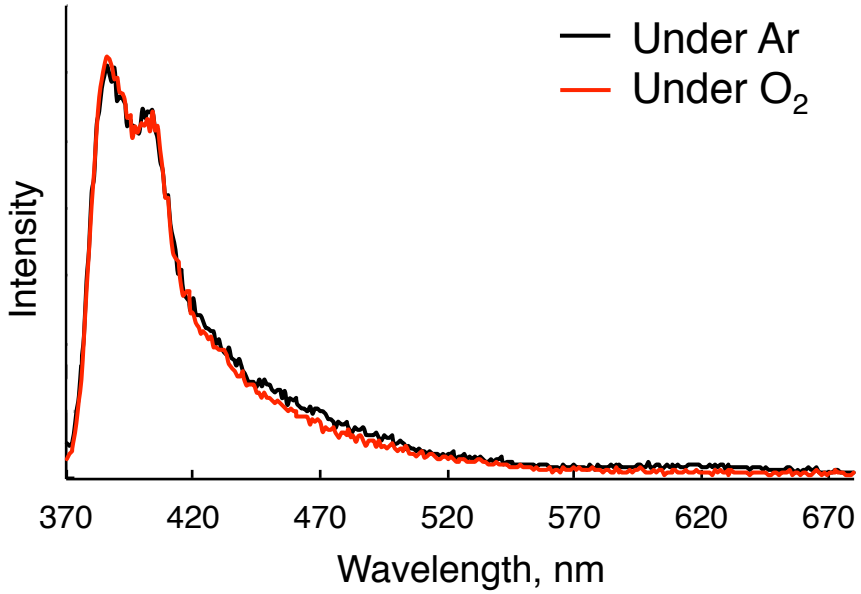

Figure S16. Emission spectra of **1**-H^+ in H_2O at pH = 1.3, adjusted by addition of TfOH, with excitation wavelength at 356 nm under Ar (black) and O_2 (1 atm; red).

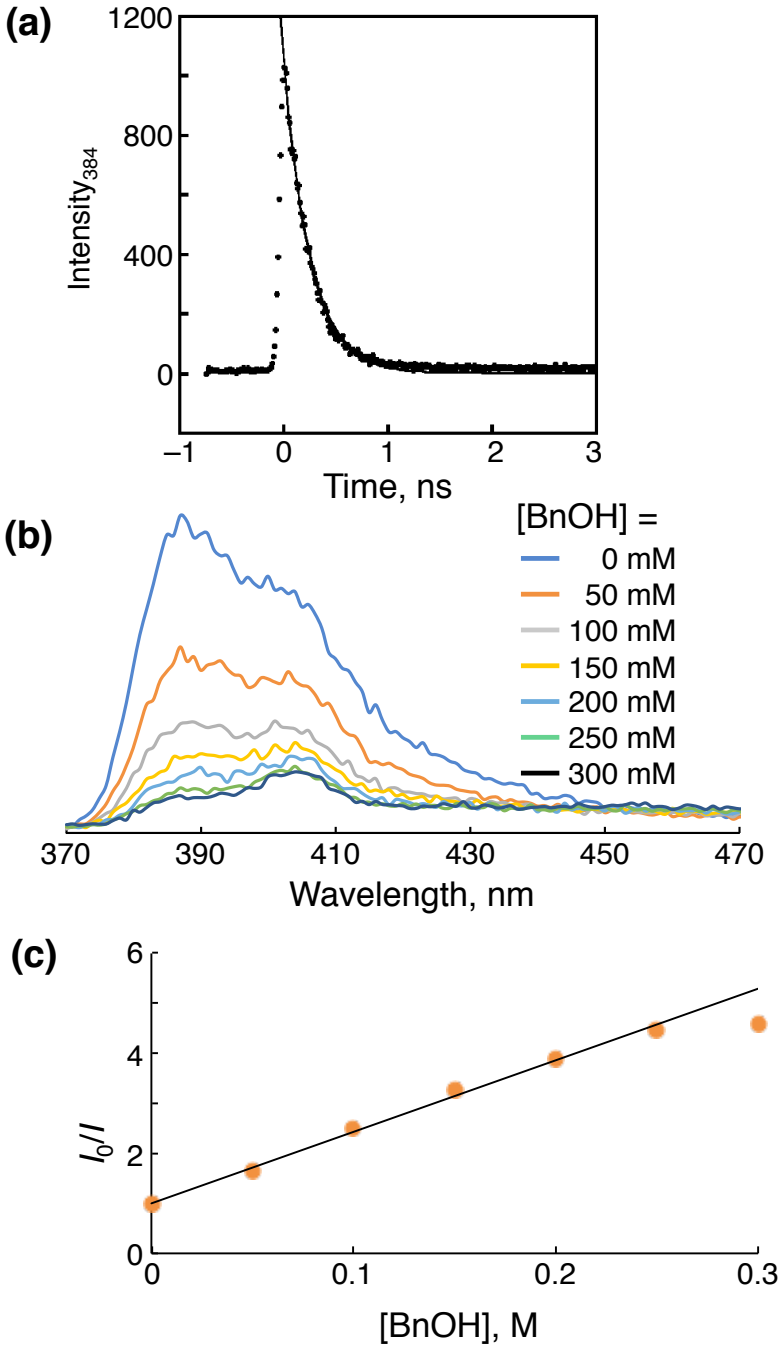

Figure S17. (a) A decay curve for the emission from **1**-H^+ in H_2O at pH = 1.3, monitored at 384 nm. Excitation wavelength: 375 nm. (b) Emission spectra of **1**-H^+ in H_2O at pH = 1.3 in the presence of BnOH: [BnOH] = 0 mM (blue), 50 (orange), 100 (gray), 150 (yellow) and 200 (light blue). (c) Stern-Volmer plots for the emission at 389 nm from **1**-H^+ in H_2O at pH = 1.3. Quencher: BnOH.

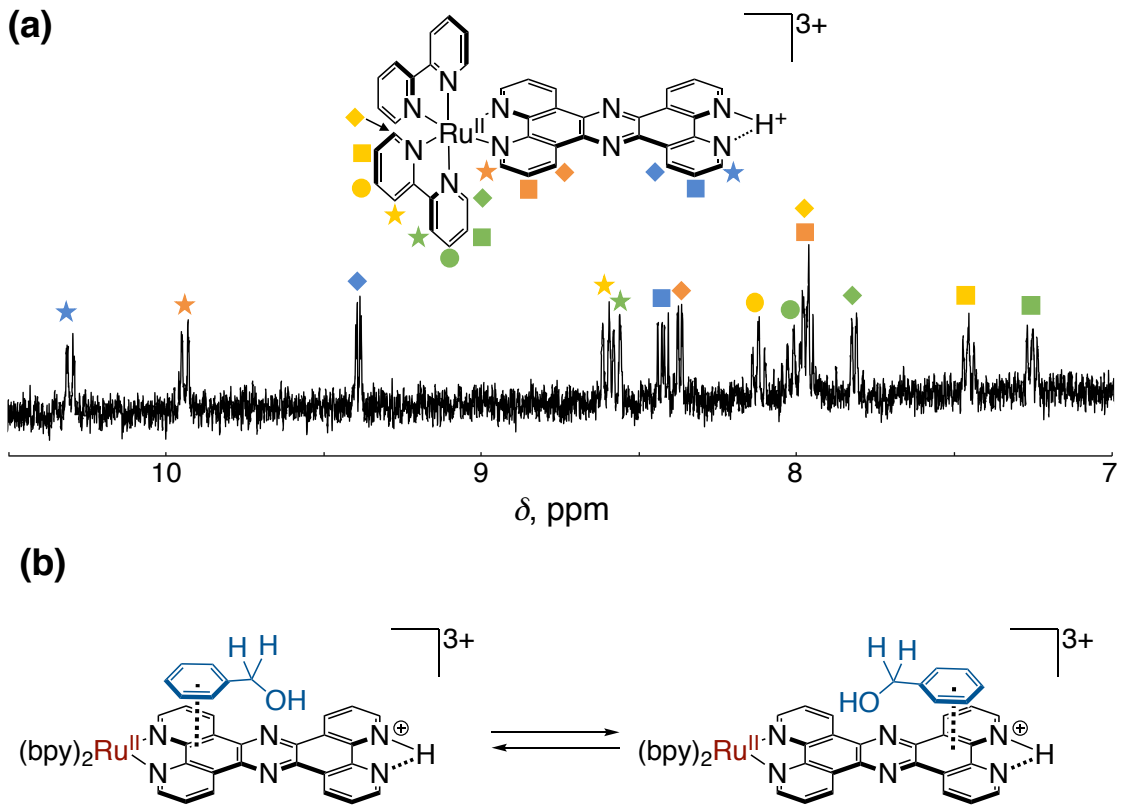

Figure S18. (a) Assignment of the ^{1}H NMR signals for **1**-H$^+$ in D_2O, whose pD was adjusted by addition of TfOH to be 1.3. (b) Plausible structures of the adduct between **1**-H$^+$ and BnOH, presumed on the basis of the well-shifted ^{1}H NMR signals in the course of the titration of an aqueous solution of **1**-H$^+$ in D_2O with BnOH (see Figure 7a).

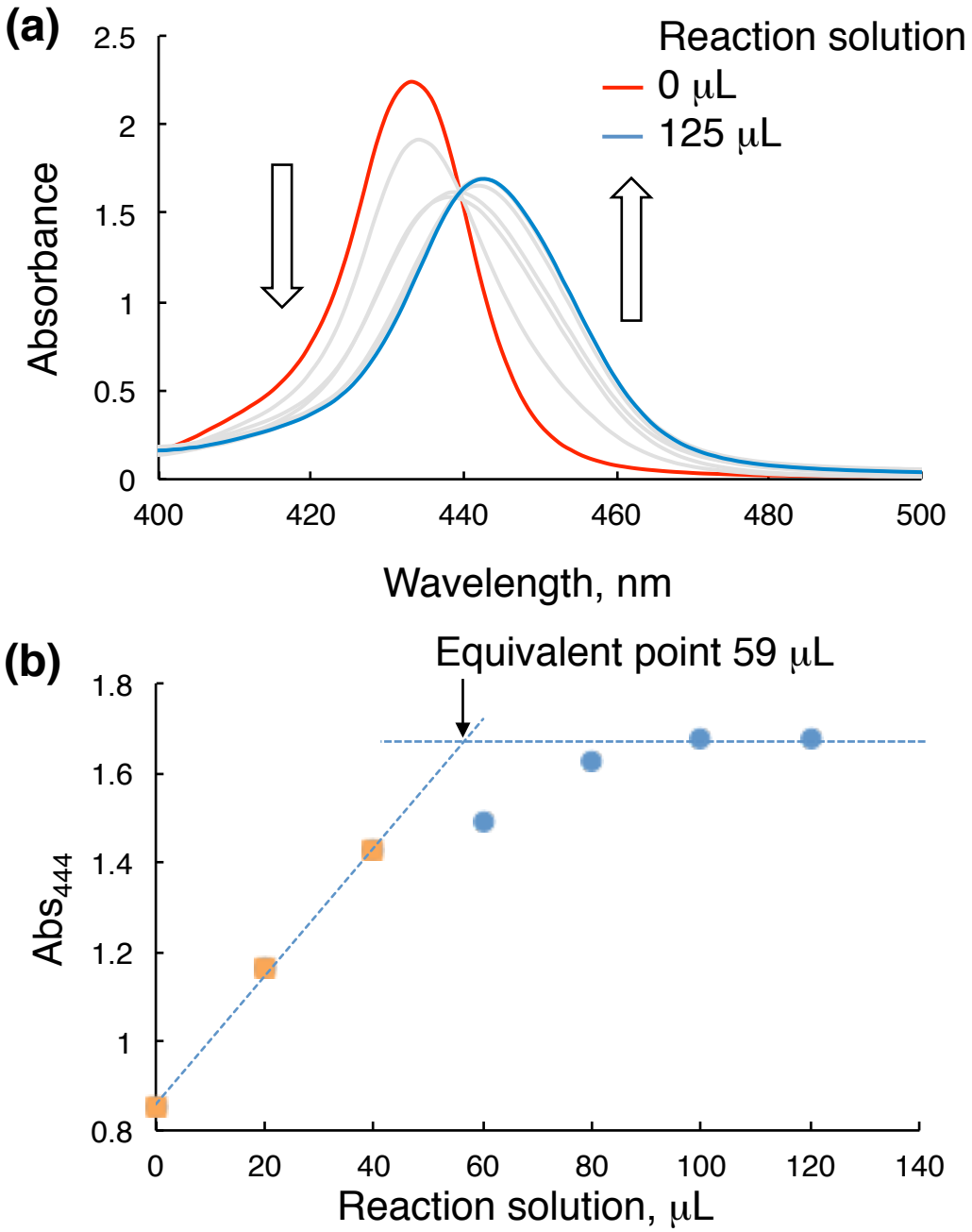

Figure S19. (a) UV-Vis spectra of TiTPyP (5 μM) in $HClO_4$ aq (0.5 M) before addition of the reaction mixture (red) and after addition of 125 μL of the reaction mixture (blue). The reaction mixture was provided by irradiation of white light (λ > 380 nm) for 10 h under O_2 (1 atm) to a solution of **1**-H^+ (0.1 mM) and BnOH (50 mM) in D_2O at pH = 1.5. After the reaction, the amount of PhCHO formed was determined to be 4.68 mM by ^1H NMR spectroscopy. (b) Absorbance change at 444 nm upon increasing the amount of the reaction mixture added, extracted from (a).

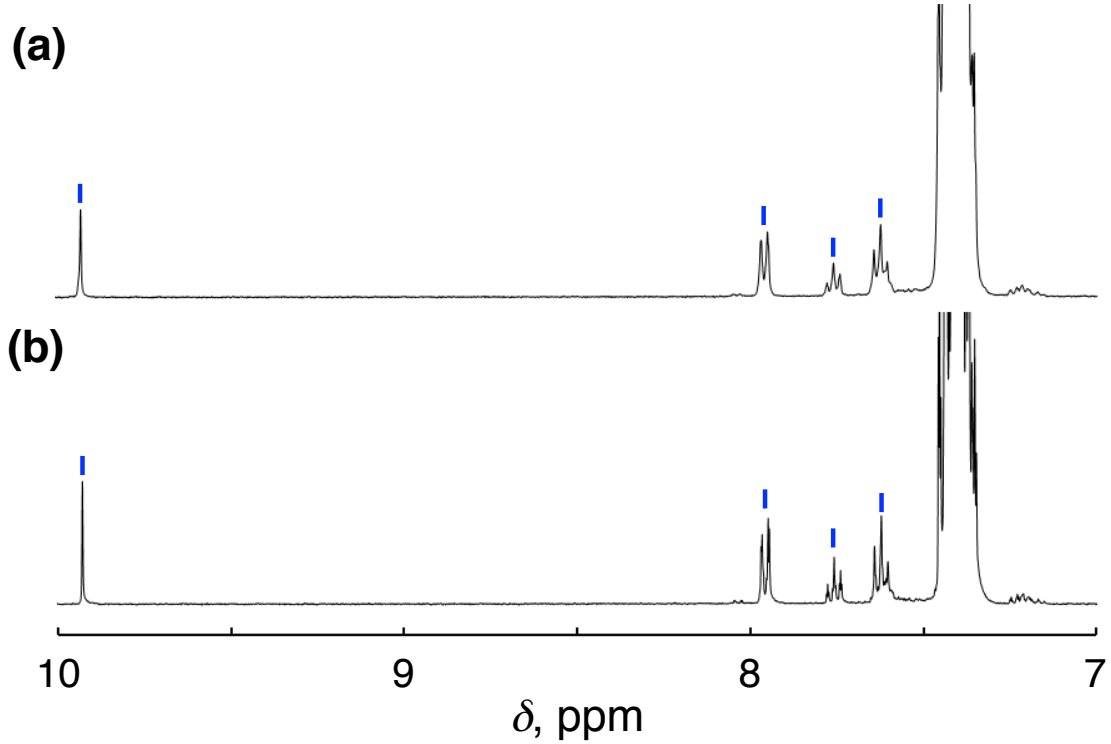

Figure S20. ^{1}H NMR spectra of a reaction solution of the photocatalytic BnOH oxidation by **1** under photo-irradiation (Xe lamp; $\lambda > 380$ nm) and O_2 (1 atm) in the absence (a) and presence (b) of MnO_2 (1 mg). Reaction conditions: [**1**] = 0.01 mM, [BnOH] = 50 mM, *T* = room temperature. Solvent: B.-R.-buffered D_2O (pD = 1.5). Reaction time: 10 h. The ^{1}H NMR signals of PhCHO are indicated by blue sticks. The calculated TONs are 216 for (a) and 220 for (b), respectively.

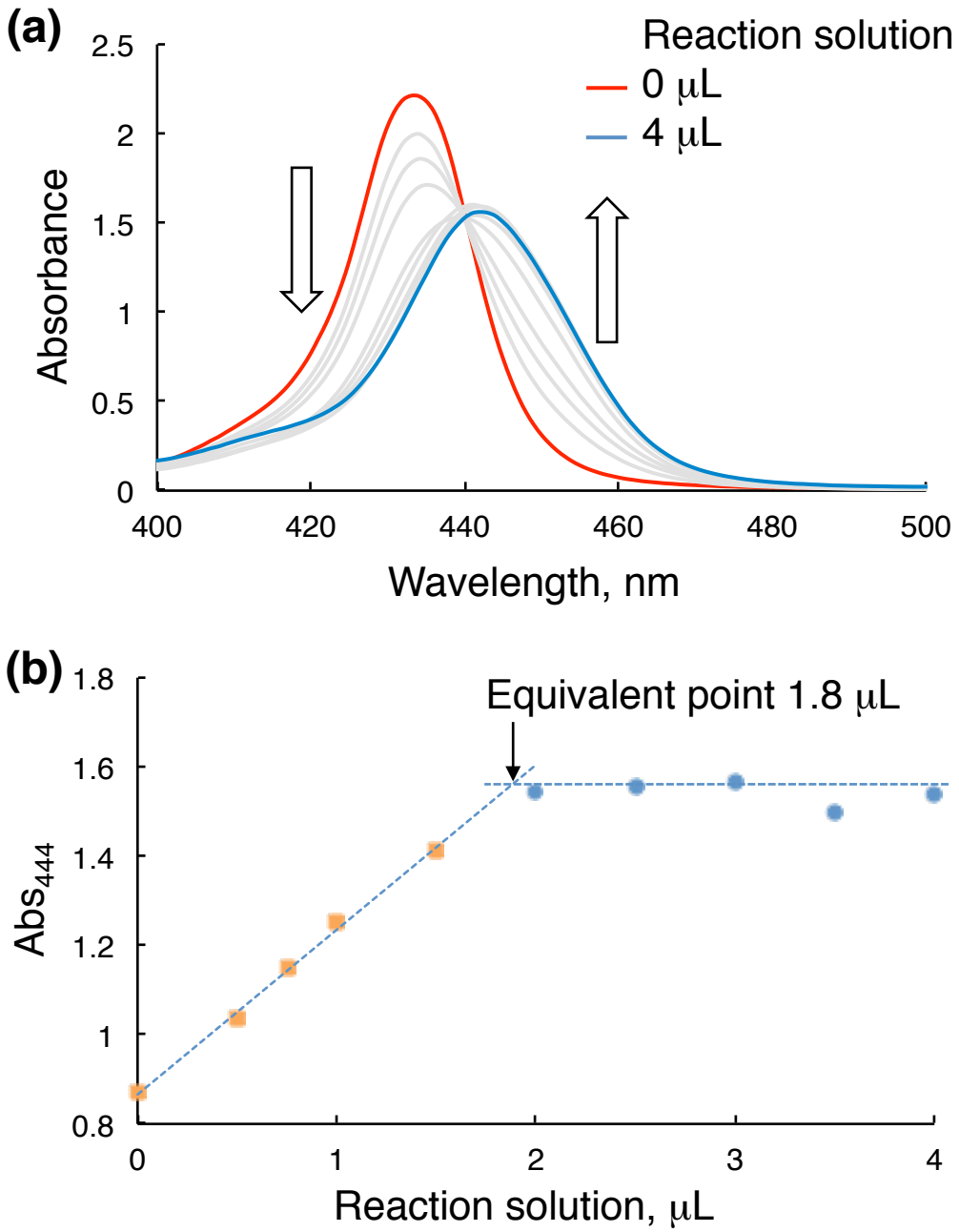

Figure S21. (a) UV-Vis spectra of TiTPyP (5 μM) in $HClO_4$ aq (0.5 M) before addition of the reaction mixture (red) and after addition of 4 μL of the reaction mixture (blue). The reaction mixture was provided by irradiation of white light ($\lambda > 380$ nm) for 10 h under Ar to a solution of **1**-H^+ (0.1 mM), BnOH (50 mM) and H_2O_2 (7.0 mM) in D_2O at pH = 1.5. After the reaction, the amount of PhCHO formed was determined to be 1.3 mM by ^1H NMR spectroscopy. (b) Absorbance change at 444 nm upon increasing the amount of the reaction mixture added, extracted from (a).

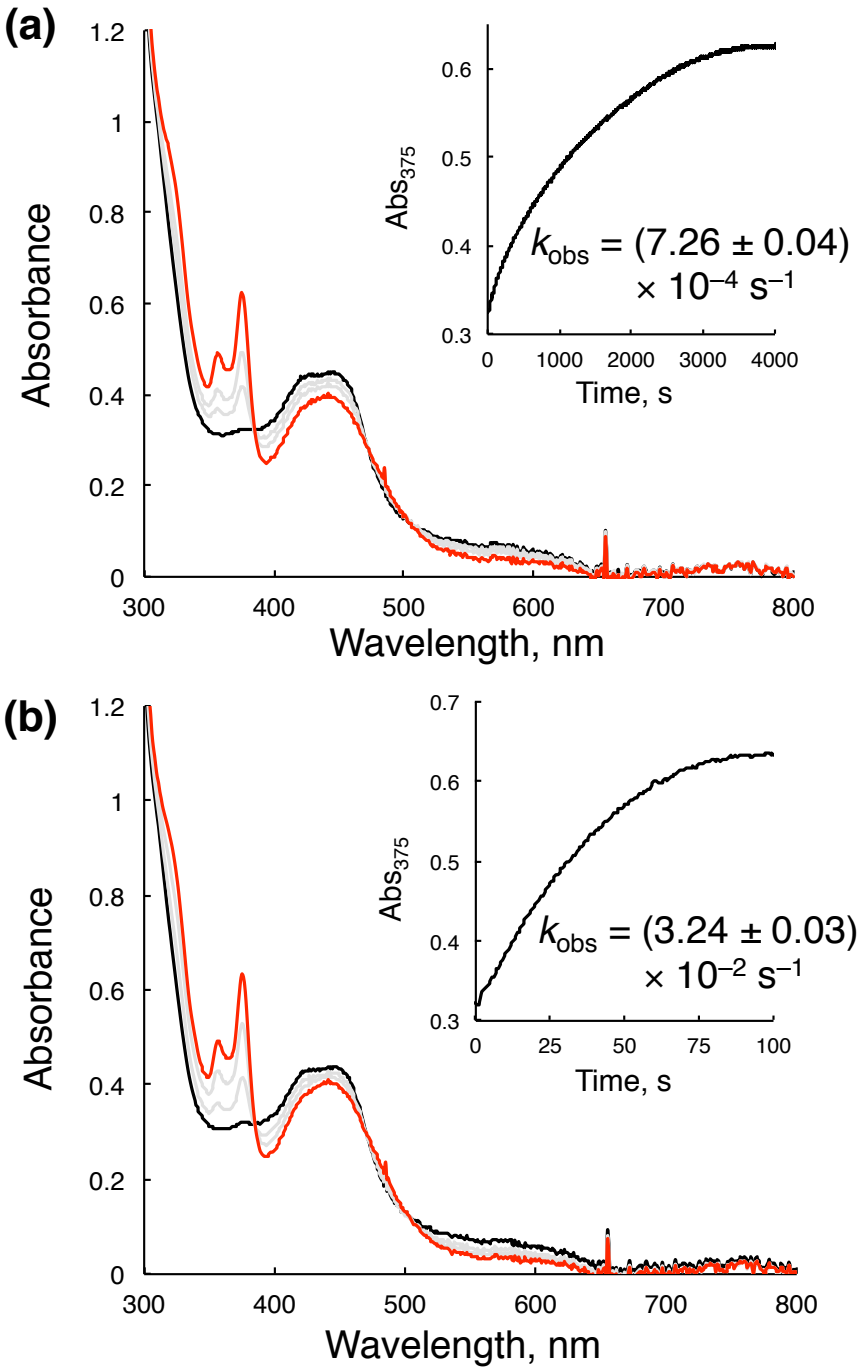

Figure S22. UV-Vis spectral changes of **2**-H^+ (0.022 mM) after addition of H_2O_2 (19 mM) (a) or O_2 (0.33 mM) (b) at 297 K: t = 0 s (red) and 4000 s (black in a) and 600 s (black in b). (Inset) Time courses of the absorbance changes at 375 nm. Complex **2**-H^+ was formed by light irradiation ($\lambda > 380$ nm) to an aqueous solution of **1**-H^+ (0.022 mM), BnOH (50 mM) and TfOH (50 mM) under Ar.

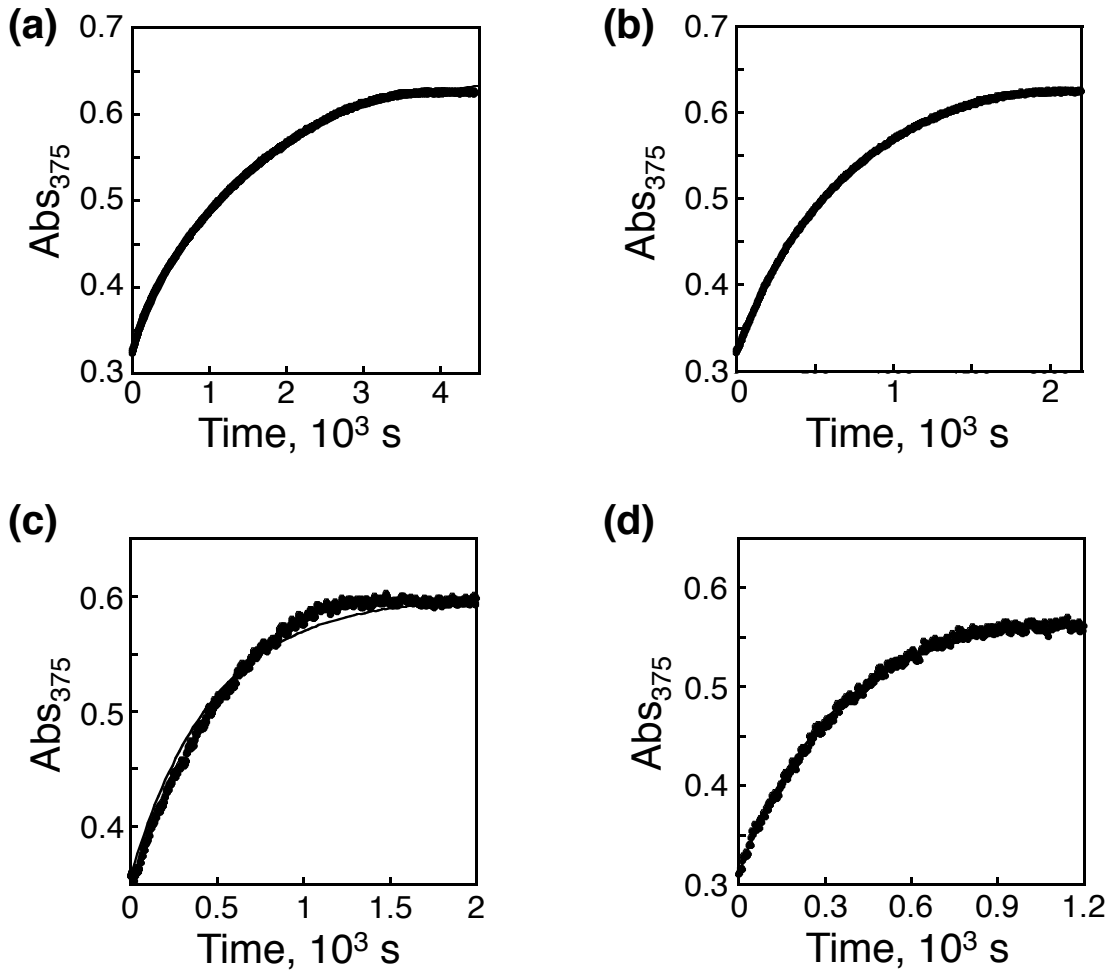

Figure S23. Time courses of the absorbance at 375 nm upon addition of H_2O_2 to an aqueous solution of **2**-H^+ (22 μM), formed by photo-irradiation to the corresponding aqueous solution of **1**-H^+, BnOH (50 mM) and TfOH (50 mM), at 297 K. Initial H_2O_2 concentration was varied as 19 (a), 39 (b), 56 (c), and 75 mM (d).

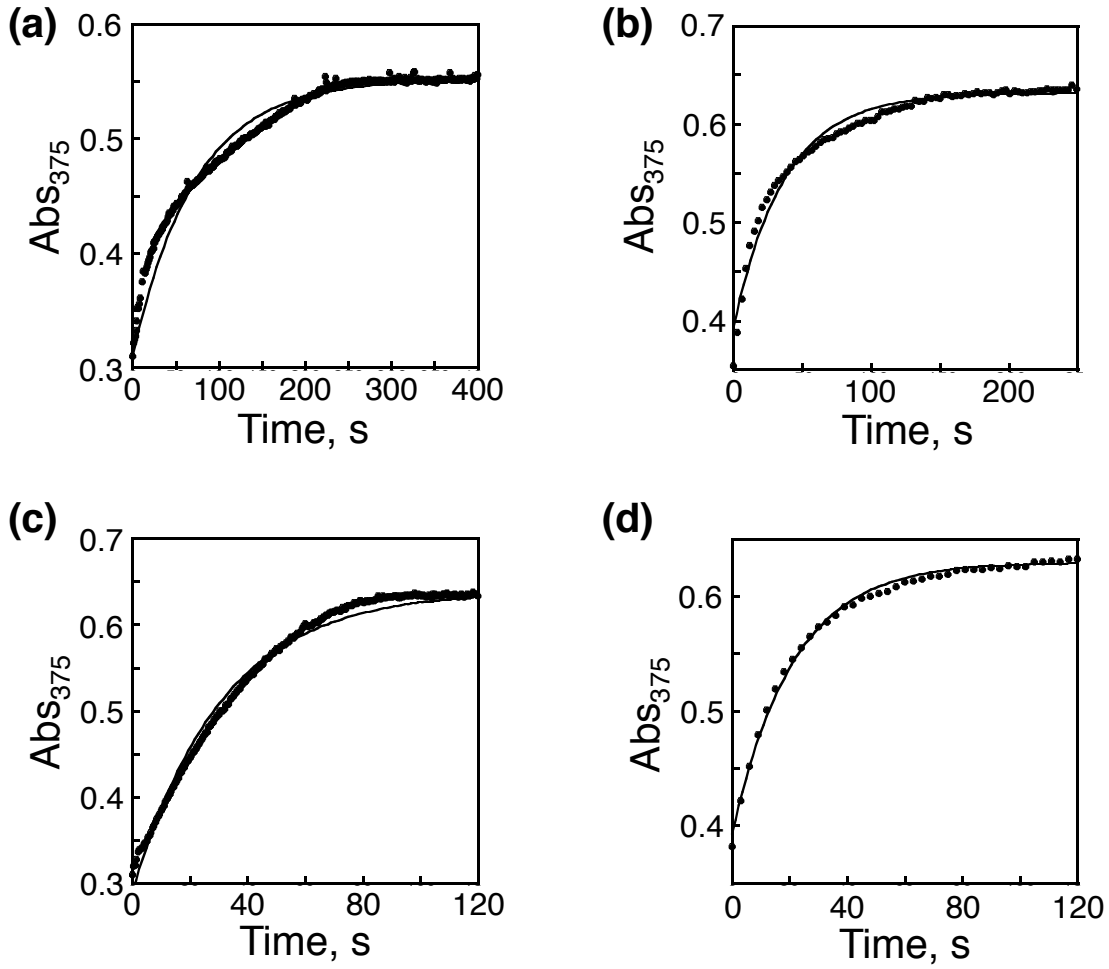

Figure S24. Time courses of the absorbance at 375 nm against the reaction time upon addition of O_2 to an aqueous solution of **2**-H^+ (22 μM), formed by photo-irradiation to the corresponding aqueous solution of **1**-H^+, BnOH (50 mM) and TfOH (50 mM), at 297 K. Initial O_2 concentration was varied as 0.33 (a), 0.50 (b), 0.66 (c), and 0.83 mM (d).

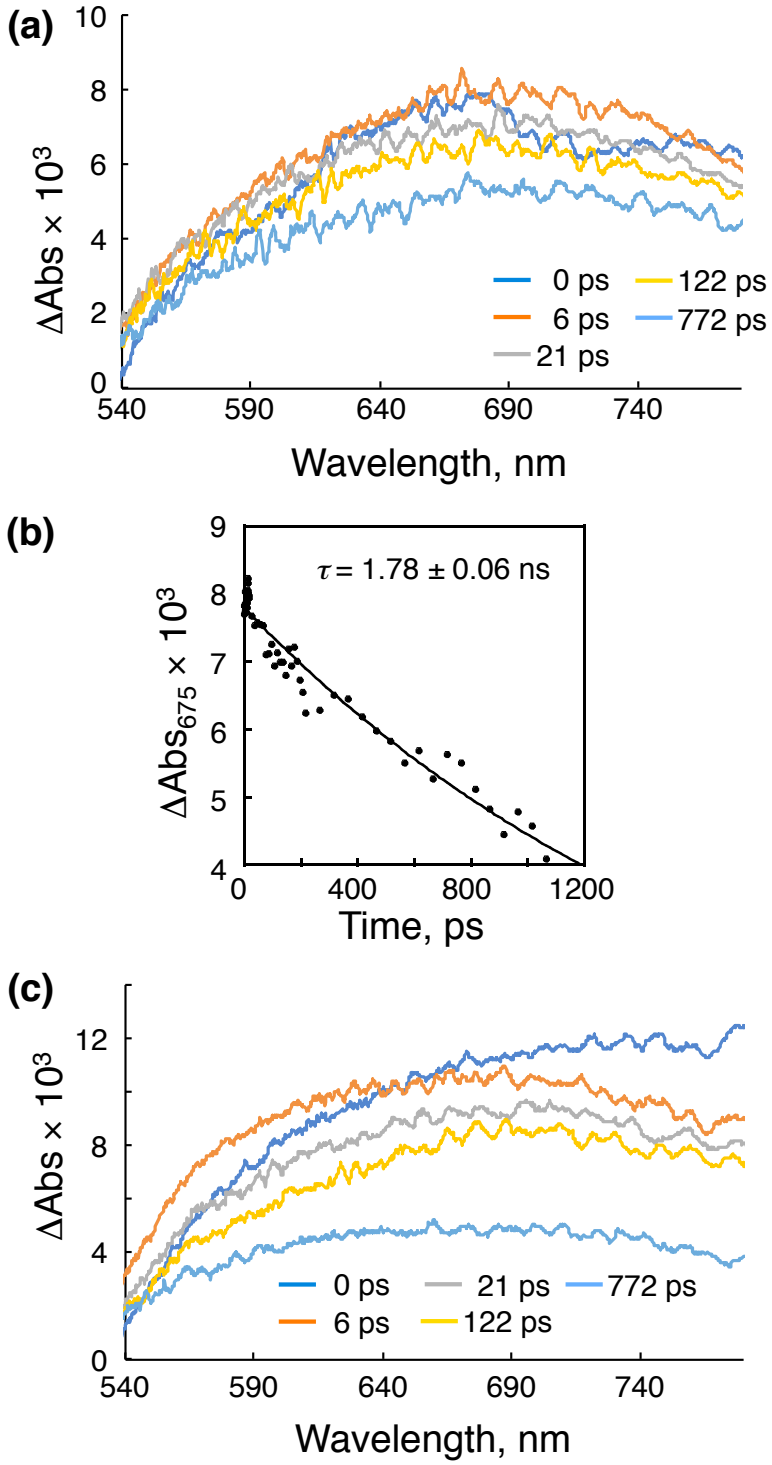

Figure S25. (a) Femto-second transient absorption spectra of **1** in an aqueous solution at pH = 7.0 upon photoexcitation at λ = 440 nm. (b) Decay of the absorbance of **1** at 675 nm in H_2O at pH = 7.0 with a single-exponential fitting curve. (c) Femto-second transient absorption spectra of **1** in an aqueous solution at pH = 7.0 upon photoexcitation at λ = 375 nm.

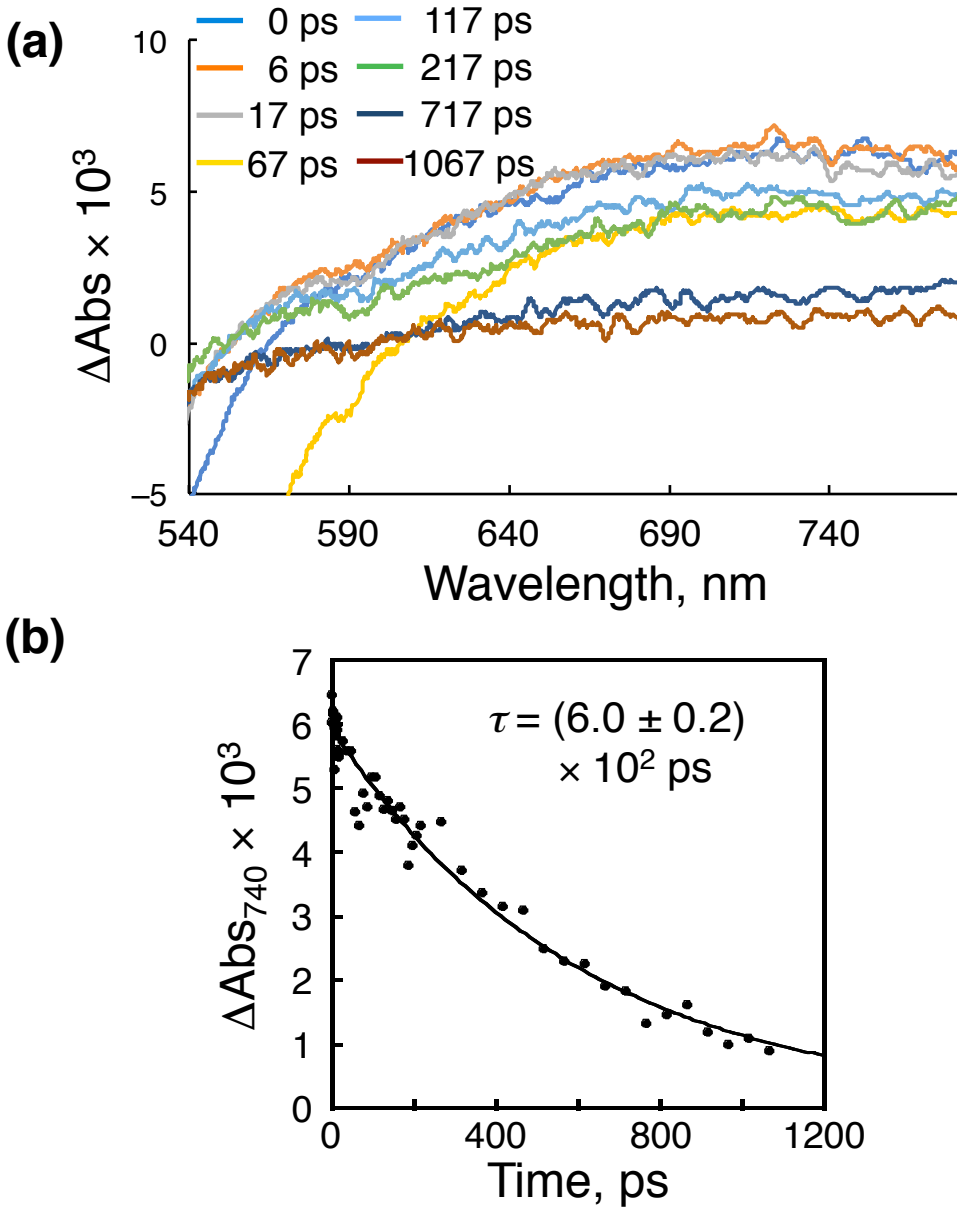

Figure S26. (a) Femto-second transient absorption spectra of **1**-H$^+$ in an aqueous solution, whose pH was controlled to be 1.3 by addition of TfOH upon photoexcitation at λ = 440 nm. (b) Decay of the transient absorption of **1**-H$^+$ at 740 nm in an aqueous solution at pH = 1.3 with a single-exponential fitting curve.

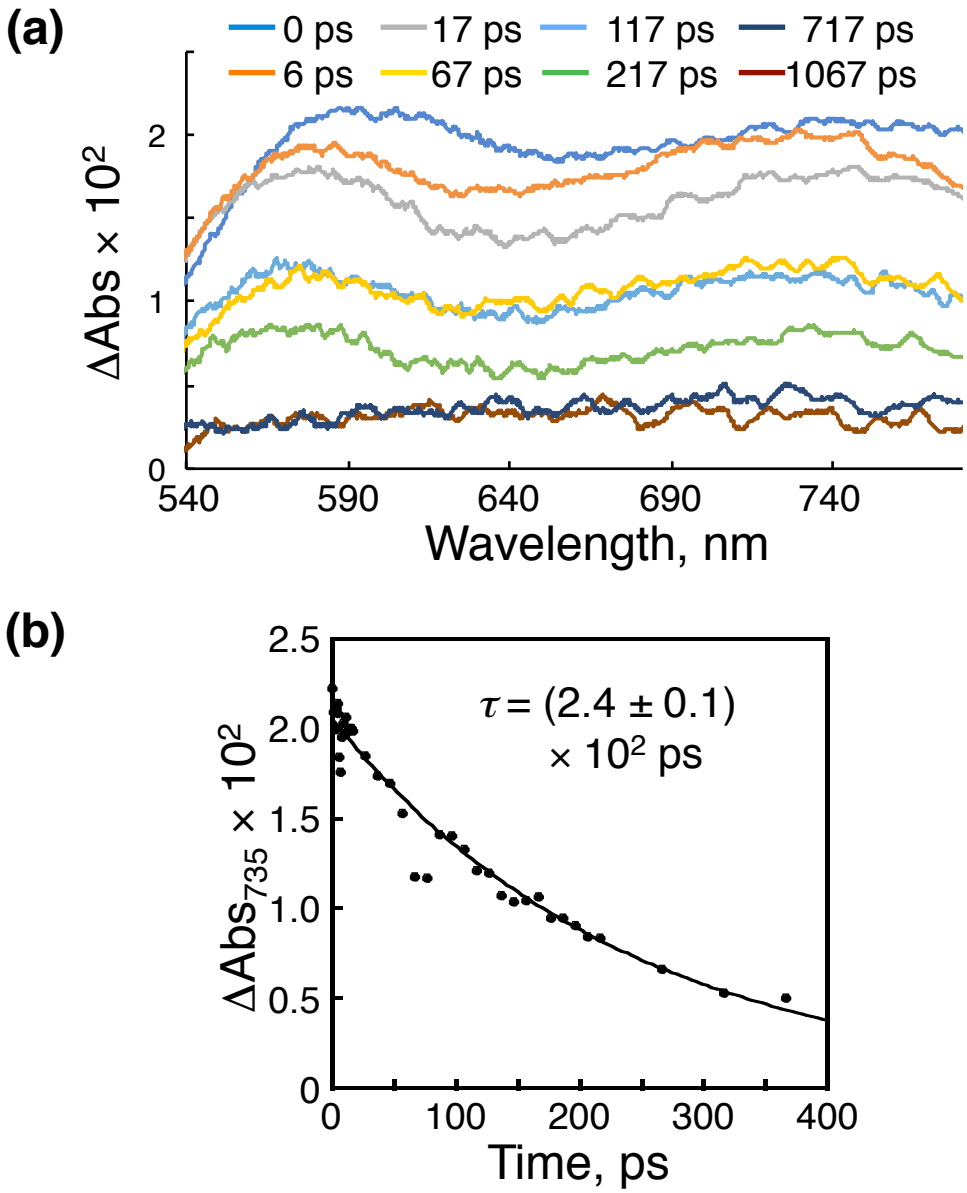

Figure S27. (a) Femto-second transient absorption spectra of **1**-H$^+$ in an aqueous solution, whose pH was adjusted to be 1.3 by addition of TfOH, and the presence of BnOH (100 mM) upon photoexcitation at λ = 375 nm. (b) Decay of the transient absorption of **1**-H$^+$ at 735 nm in an aqueous solution at pH = 1.3 containing BnOH (100 mM) with a single-exponential fitting curve.

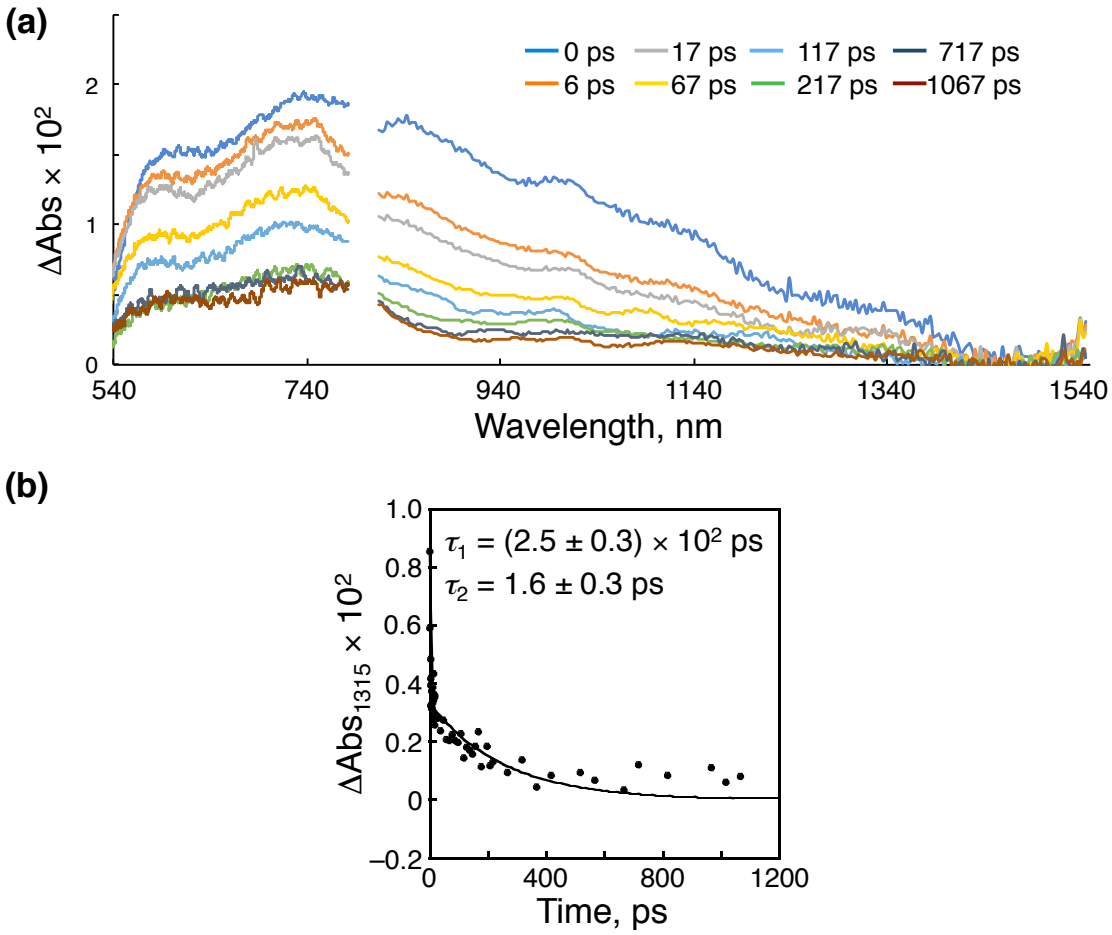

Figure S28. (a) Femto-second transient absorption spectra of **1**-H^+ in an aqueous solution at pH = 1.3 in the absence of BnOH upon photoexcitation at λ = 375 nm. (b) Decay of the absorbance at 1315 nm with a double- exponential fitting curve.

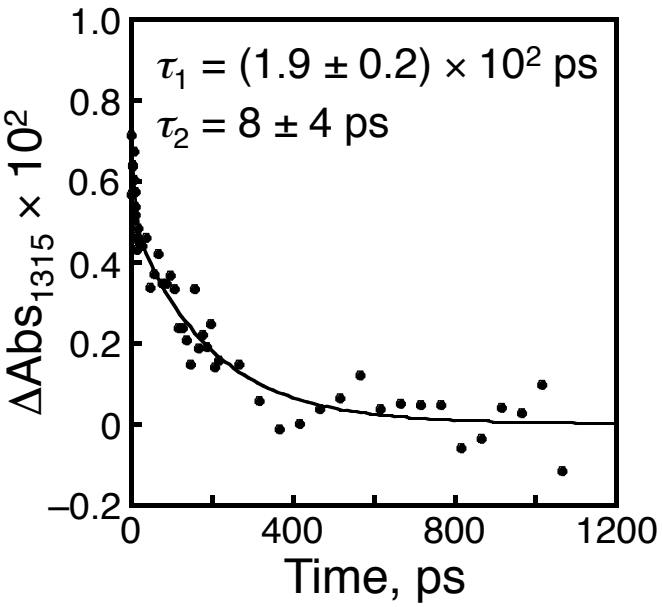

Figure S29. Decay of the absorption of **1**-H$^+$ at 1315 nm in an aqueous solution containing BnOH (100 mM) at pH = 1.3 with a double-exponential fitting curve.

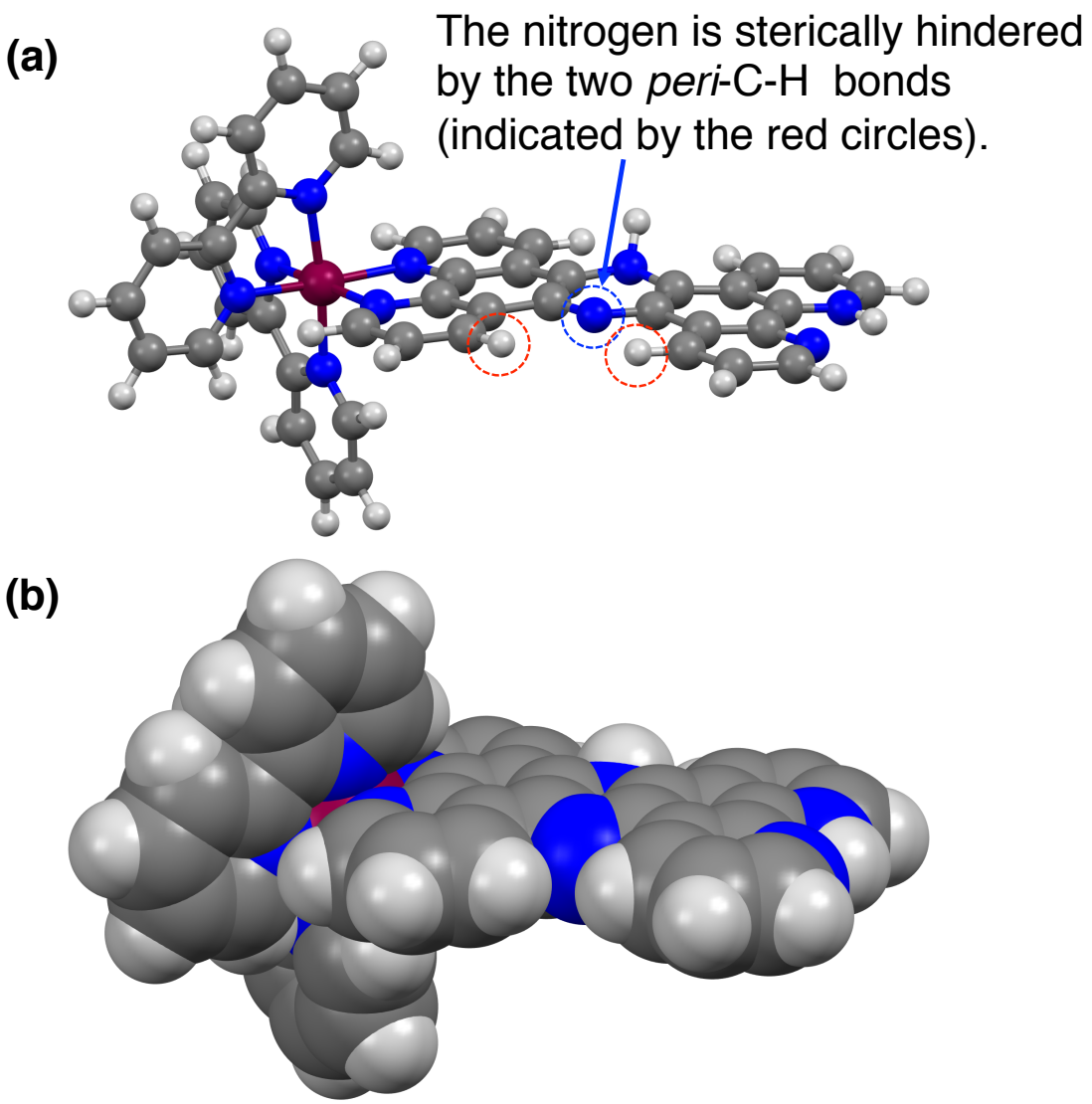

Figure S30. The DFT-optimized structure of $[Ru^{II}(H^{-}\text{-tpphz-}H^{+})(bpy)_2]^{2+}$ in the closed singlet state, which is more stable than the triplet state, derived from **1**-H^{+} through formal hydride transfer: (a) ball-and-stick and (b) space-filling models.

Table S1. Redox Potentials of **1** and **1**-H^+ in CH_3CN at Room Temperature

	E (vs Fc/Fc^+), V			
	bpy/$bpy^{\bullet-}$	bpy/$bpy^{\bullet-}$	tpphz/$tpphz^{\bullet-}$ or $Htpphz^+$/$Htpphz^{\bullet}$	Ru^{III}/Ru^{II}
1	–1.99	–1.78	–1.36	+0.94
1-H^+ [a]	–1.09	–0.83	–0.48	+0.97

Electrolyte: $TBAPF_6$ (0.1 M). WE: glassy carbon disk. CE: Pt wire. RE: $Ag/AgNO_3$. [a]For protonation of **1**, TfOH (0.5 mM) was added.

Table S2. Apparent Rate Constants for the Reaction of **2**-H^+ with H_2O_2 or O_2

Oxidant	$k_{obs} \times 10^3$, s^{-1} ([Oxidant], mM)			
H_2O_2	0.726 ± 0.002 (19)	1.517 ± 0.005 (39)	2.08 ± 0.01 (56)	3.00 ± 0.02 (75)
O_2	14 ± 2 (0.33)	27 ± 1 (0.50)	32.4 ± 0.3 (0.66)	47 ± 1 (0.83)

Table S3. The Crystallographic Data of [**1**-H^+]·$(OTf)_3$

	[**1**-H^+]·$(OTf)_3$
formula	$C_{44}H_{32}N_{10}Ru \cdot 3CF_3SO_3 \cdot 7.5H_2O$
formula wt	1384.19
cryst syst	triclinic
space group	$P\bar{1}$
a, Å	12.1750(18)
b, Å	12.1917(18)
c, Å	21.691(3)
α, °	85.134(2)
β, °	77.352(2)
γ, °	60.119(2)
V, Å^3	2722.8(7)
Z	2
*R*1 ($I > 2\sigma(I)$)	0.0645
*wR*2 (all)	0.1829
GOF	1.036

Table S4. Cartesian coordinates of an optimized structure of the adduct of **1**-H^+ with BnOH.

Atom	X	Y	Z
C	3.701866000	-3.651720000	-1.892674000
C	3.753645000	-2.541590000	-1.045821000
N	2.910783000	-1.484875000	-1.226527000
C	2.017172000	-1.519416000	-2.232976000
C	1.919159000	-2.596702000	-3.105727000
C	2.777248000	-3.681860000	-2.933467000
C	4.691279000	-2.409271000	0.084877000
N	4.563322000	-1.263935000	0.814693000
C	5.377147000	-1.059971000	1.868326000
C	6.348574000	-1.978056000	2.248956000
C	6.488037000	-3.152746000	1.510642000
C	5.651201000	-3.367805000	0.419337000
Ru	3.096987000	0.059573000	0.160908000
N	4.549032000	1.133735000	-0.869565000
C	5.047213000	2.224528000	-0.219767000
C	6.035113000	3.018780000	-0.807355000
C	6.518768000	2.692889000	-2.071267000
C	6.003503000	1.574187000	-2.725185000
C	5.022526000	0.821120000	-2.091128000
C	4.464480000	2.483838000	1.110076000
N	3.526204000	1.582545000	1.518644000
C	2.940324000	1.740739000	2.721073000
C	3.258611000	2.791740000	3.572971000
C	4.218145000	3.718317000	3.166092000
C	4.825058000	3.561156000	1.923348000
N	1.530126000	-0.816371000	1.233482000
C	1.600183000	-1.835929000	2.100709000
C	0.465414000	-2.371077000	2.721236000
C	-0.783998000	-1.842406000	2.438305000
C	-0.878040000	-0.771874000	1.532572000
C	0.305843000	-0.287229000	0.949495000
C	0.280053000	0.809496000	0.008276000
C	-0.929340000	1.433334000	-0.344274000
C	-2.169957000	0.924386000	0.226975000
C	-2.146386000	-0.158099000	1.155112000
N	-3.324798000	1.471110000	-0.160954000

C	-4.451665000	0.969401000	0.340340000
C	-4.432341000	-0.104626000	1.280079000
N	-3.277186000	-0.643138000	1.674981000
N	1.478506000	1.189069000	-0.520953000
C	1.500536000	2.208985000	-1.390847000
C	0.339373000	2.887218000	-1.779532000
C	-0.887038000	2.501189000	-1.259586000
C	-5.722025000	1.521710000	-0.111764000
C	-6.903706000	0.966711000	0.396763000
C	-6.909774000	-0.122172000	1.354456000
C	-5.681197000	-0.651270000	1.796481000
N	-8.114314000	-0.572608000	1.752391000
C	-8.135861000	-1.580778000	2.618044000
C	-6.968496000	-2.184744000	3.124512000
C	-5.732180000	-1.718704000	2.712042000
C	-5.818456000	2.558622000	-1.055218000
C	-7.064970000	3.017152000	-1.465490000
C	-8.212211000	2.437061000	-0.932998000
N	-8.095287000	1.449164000	-0.033906000
O	-0.835950000	-0.447524000	-3.144235000
C	-1.504789000	-1.436810000	-2.368526000
H	2.470088000	2.480011000	-1.789968000
H	-1.807196000	2.996653000	-1.545479000
H	-1.684171000	-2.234759000	2.895783000
H	2.589678000	-2.228114000	2.301592000
H	-4.907478000	2.984180000	-1.459127000
H	-7.161266000	3.812710000	-2.192823000
H	-9.216778000	2.736109000	-1.202120000
H	-9.115408000	-1.933515000	2.928857000
H	-7.049381000	-3.005840000	3.827597000
H	-4.808924000	-2.156735000	3.072579000
H	5.230628000	-0.136039000	2.413087000
H	6.977040000	-1.767296000	3.106213000
H	5.747405000	-4.273733000	-0.165191000
H	4.373687000	-4.486996000	-1.742494000
H	1.179373000	-2.570329000	-3.897063000
H	1.357817000	-0.668323000	-2.338797000
H	4.590926000	-0.053568000	-2.560789000
H	6.349574000	1.281562000	-3.709518000
H	6.425375000	3.883204000	-0.285842000

H	5.570890000	4.272298000	1.592441000
H	2.760009000	2.873782000	4.531559000
H	2.204326000	0.995301000	2.995179000
H	0.581258000	-3.195565000	3.414595000
H	0.415517000	3.703362000	-2.487985000
H	7.235741000	-3.891220000	1.777883000
H	2.729735000	-4.539990000	-3.594753000
H	7.285130000	3.303549000	-2.535570000
H	4.491520000	4.551278000	3.804276000
H	-8.918783000	0.997576000	0.371443000
H	-1.072111000	0.424767000	-2.798865000
H	-1.108515000	-1.471225000	-1.341947000
C	-3.014309000	-1.289987000	-2.320993000
H	-1.239908000	-2.394997000	-2.828743000
C	-3.750473000	-2.060512000	-1.410816000
C	-5.142994000	-1.971577000	-1.369233000
C	-5.816093000	-1.096290000	-2.227545000
C	-5.086819000	-0.314818000	-3.125648000
C	-3.693577000	-0.416393000	-3.177252000
H	-3.232353000	-2.729774000	-0.728351000
H	-5.700578000	-2.575418000	-0.659632000
H	-6.898648000	-1.019875000	-2.189860000
H	-5.601128000	0.374739000	-3.788489000
H	-3.130265000	0.179562000	-3.887805000

Table S5. Cartesian coordinates of an optimized structure of the intermediate formed by formal hydride transfer from BnOH to **1**-H^+

Atom	X	Y	Z
C	-3.868051	2.968942	-2.812846
C	-3.700681	2.127955	-1.709305
N	-2.805535	1.099475	-1.742965
C	-2.076636	0.897171	-2.857513
C	-2.202481	1.698124	-3.986297
C	-3.113817	2.753722	-3.962738
C	-4.449150	2.265109	-0.445954
N	-4.111636	1.371301	0.527663
C	-4.742477	1.424670	1.716725
C	-5.729573	2.362009	1.996568
C	-6.083724	3.279807	1.007756
C	-5.436879	3.228415	-0.223536
Ru	-2.642796	-0.007120	0.011373
N	-4.117934	-1.405025	-0.427208
C	-4.389264	-2.304906	0.561324
C	-5.372534	-3.283094	0.390579
C	-6.084501	-3.342534	-0.803808
C	-5.798790	-2.417521	-1.807918
C	-4.811878	-1.465904	-1.580221
C	-3.577289	-2.157606	1.783385
N	-2.696867	-1.116041	1.771243
C	-1.914180	-0.903634	2.846705
C	-1.969262	-1.706751	3.979604
C	-2.865370	-2.775360	4.002654
C	-3.675272	-3.001058	2.893372
N	-1.026803	1.211196	0.548357
C	-1.055040	2.415599	1.123346
C	0.116870	3.131659	1.416517
C	1.348439	2.584820	1.102996
C	1.411661	1.314964	0.492239
C	0.186606	0.660398	0.228843
C	0.175334	-0.626371	-0.382704
C	1.405519	-1.253025	-0.724993
C	2.628473	-0.566103	-0.496932
C	2.670678	0.691560	0.114524
N	3.843102	-1.185057	-0.915390

C	5.043290	-0.564625	-0.443625
C	4.974191	0.706962	0.152319
N	3.822314	1.366904	0.397848
N	-1.040792	-1.201732	-0.614475
C	-1.089076	-2.415849	-1.169712
C	0.080969	-3.117936	-1.517725
C	1.319346	-2.549047	-1.303482
C	6.263727	-1.253397	-0.595472
C	7.476730	-0.614818	-0.208837
C	7.471344	0.698135	0.367758
C	6.225830	1.343605	0.554887
N	8.666542	1.240839	0.703044
C	8.660693	2.452527	1.239677
C	7.479039	3.188467	1.473396
C	6.261585	2.631706	1.130557
C	6.383761	-2.568314	-1.140941
C	7.620557	-3.167920	-1.284528
C	8.781529	-2.483794	-0.901381
N	8.657296	-1.252193	-0.383840
H	-2.073058	-2.835674	-1.338690
H	2.226785	-3.086181	-1.554596
H	2.274094	3.106451	1.315196
H	-2.034122	2.815348	1.359825
H	5.484285	-3.102281	-1.424815
H	7.711523	-4.168095	-1.690260
H	9.782095	-2.882964	-0.990808
H	9.628394	2.873793	1.502383
H	7.539421	4.175829	1.918269
H	5.326755	3.155925	1.291478
H	-4.432460	0.693462	2.452734
H	-6.205527	2.364137	2.970175
H	-5.702250	3.931199	-1.002880
H	-4.576661	3.786491	-2.776981
H	-1.593827	1.492608	-4.859091
H	-1.383157	0.066112	-2.827418
H	-4.553680	-0.729272	-2.330698
H	-6.327205	-2.425286	-2.754037
H	-5.583691	-3.991112	1.181620
H	-4.373550	-3.828254	2.893607
H	-1.318863	-1.492720	4.819597

H	-1.235451	-0.062573	2.781773
H	0.036609	4.104419	1.888046
H	-0.010824	-4.107525	-1.951238
H	-6.851144	4.024064	1.189547
H	-3.236559	3.400923	-4.824139
H	-6.849181	-4.098177	-0.945777
H	-2.933637	-3.424337	4.868736
H	9.475905	-0.721148	-0.082746
H	3.862735	-1.350086	-1.920717